

# PiTP Summer School 2009

## *Plan for my lectures*

Volker Springel

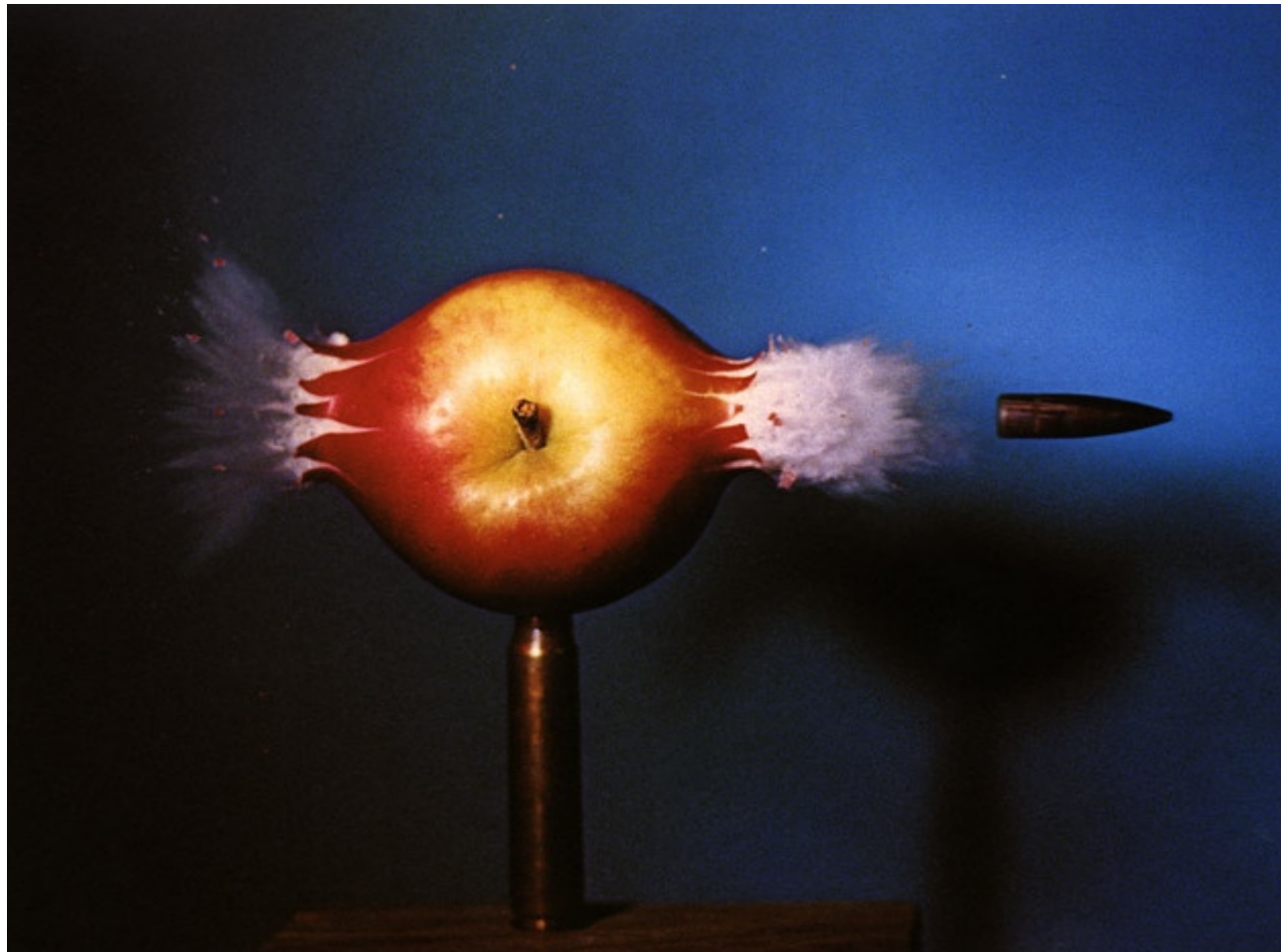
- Lecture 1 ▶ **Basics of collisionless dynamics and the N-body approach**
- Lecture 2 ▶ **Gravitational solvers suitable for collisionless dynamics, parallelization**
- Lecture 3 ▶ **More parallelization, Introduction to smoothed particle hydrodynamics**
- Lecture 4 ▶ **Algorithmic aspects of SPH, caveats, applications**
- Lecture 5 ▶ **Comparison of SPH to finite volume methods, Moving-mesh hydrodynamics**



# Example applications of SPH and collisionless dynamics in cosmology

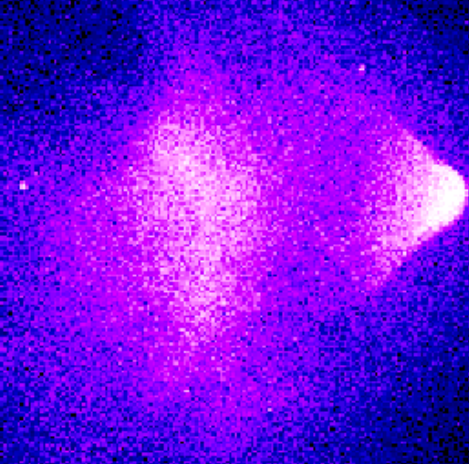
# An example application of SPH and collisionless dynamics in cosmology

## The bullet cluster



1E 0657-56

500 ks  $z=0.3$



NASA Press Release Aug 21, 2006:

## 1E 0657-56: NASA Finds Direct Proof of Dark Matter

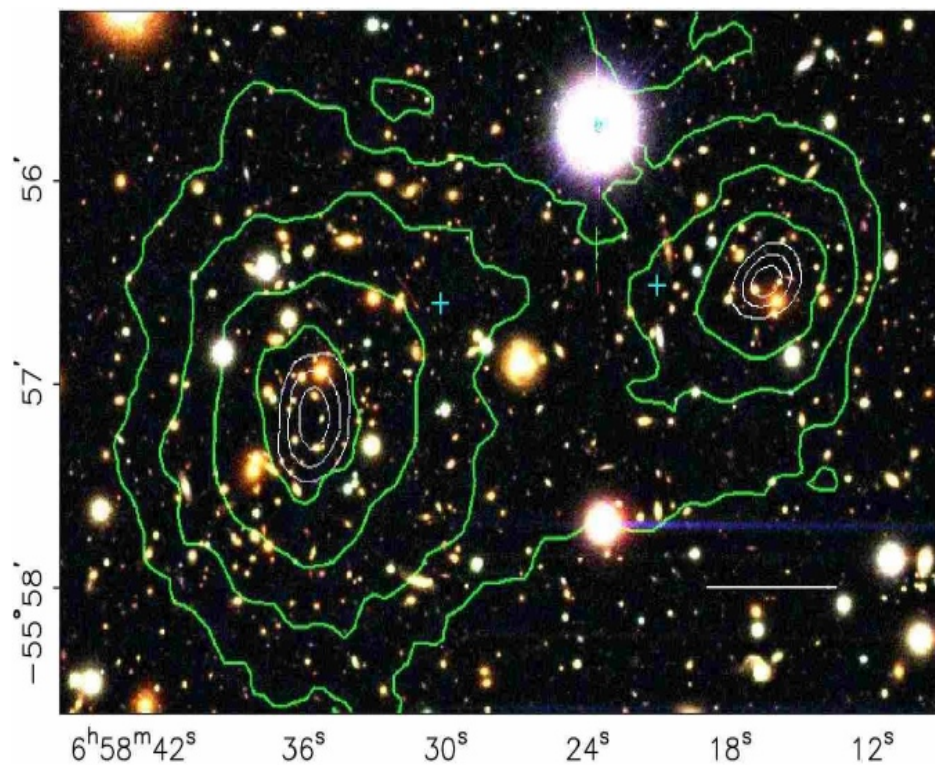


# New weak lensing mass reconstructions have confirmed an offset between mass peaks and X-ray emission

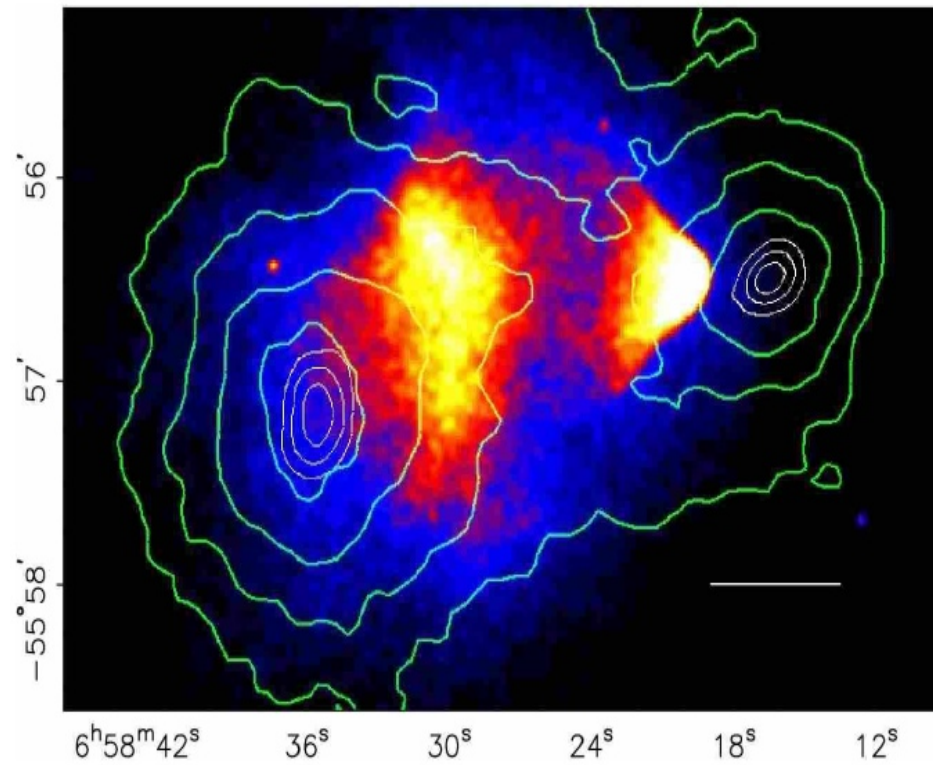
## MASS CONTOURS FROM LENSING COMPARED TO X-RAY EMISSION

Clowe et al. (2006)

Magellan Optical Image



500 ksec Chandra exposure

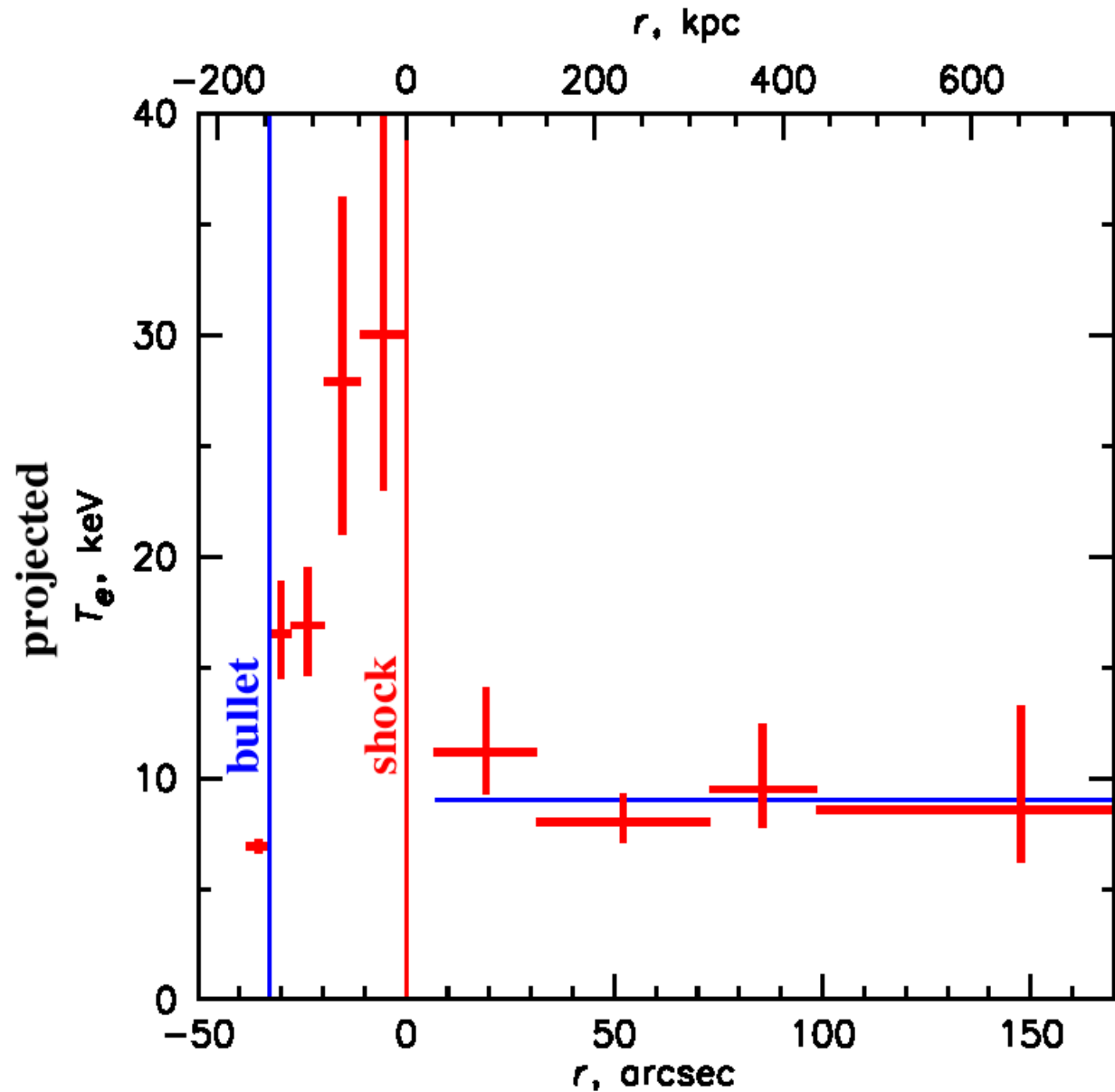


weak lensing mass contours overlaid

The temperature profile through the nose of the shock shows a strong shock and a cold front

**X-RAY TEMPERATURE PROFILE FROM CHANDRA OBSERVATIONS**

Markevitch et al. (2006)



Fitting the density jump in the X-ray surface brightness profile allows a measurement of the shock's Mach number

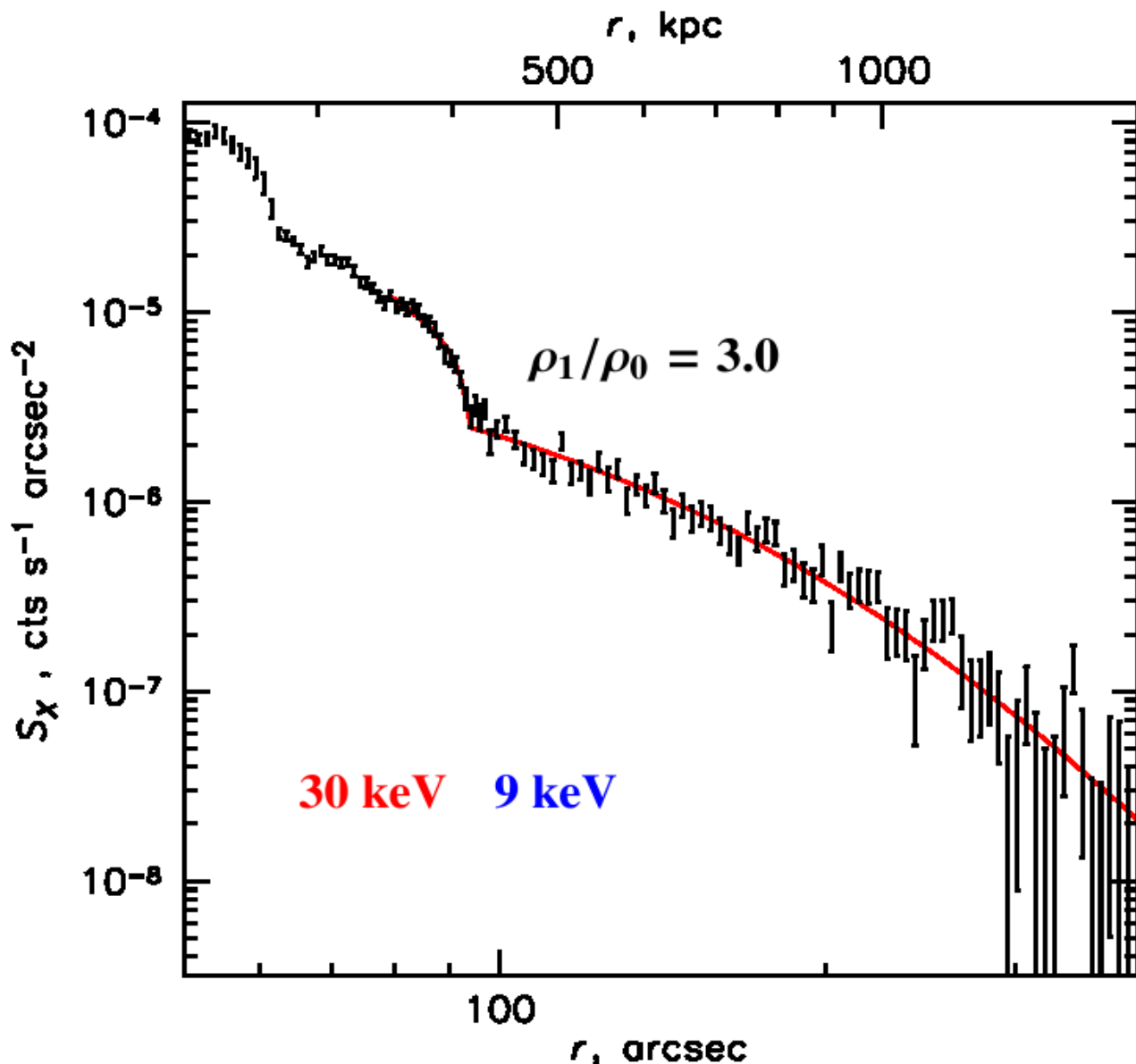
### X-RAY SURFACE BRIGHTNESS PROFILE

Markevitch et al. (2006)

shock strength:  
 **$M = 3.0 \pm 0.4$**

shock velocity:  
 **$v_s = 4700 \text{ km/s}$**

Usually, shock velocity  
has been identified with  
velocity of the bullet.





# How rare is the bullet cluster?

## DISTRIBUTION OF VELOCITIES OF THE MOST MASSIVE SUBSTRUCTURE IN THE MILLENNIUM RUN

### Hayashi & White (2006)

Adopted mass model from Clowe et al. (2004):

NFW-Halo with:

$$M_{200} = 2.96 \times 10^{15} M_{\odot}$$

$$R_{200} = 2.25 \text{ Mpc}$$

$$V_{200} = 2380 \text{ km/sec}$$

$$V_{\text{shock}} = 4500 \text{ km/sec}$$

$$V_{\text{sub}}/V_{\text{shock}} = 1.9 \quad \text{chance: } 10^{-2}$$

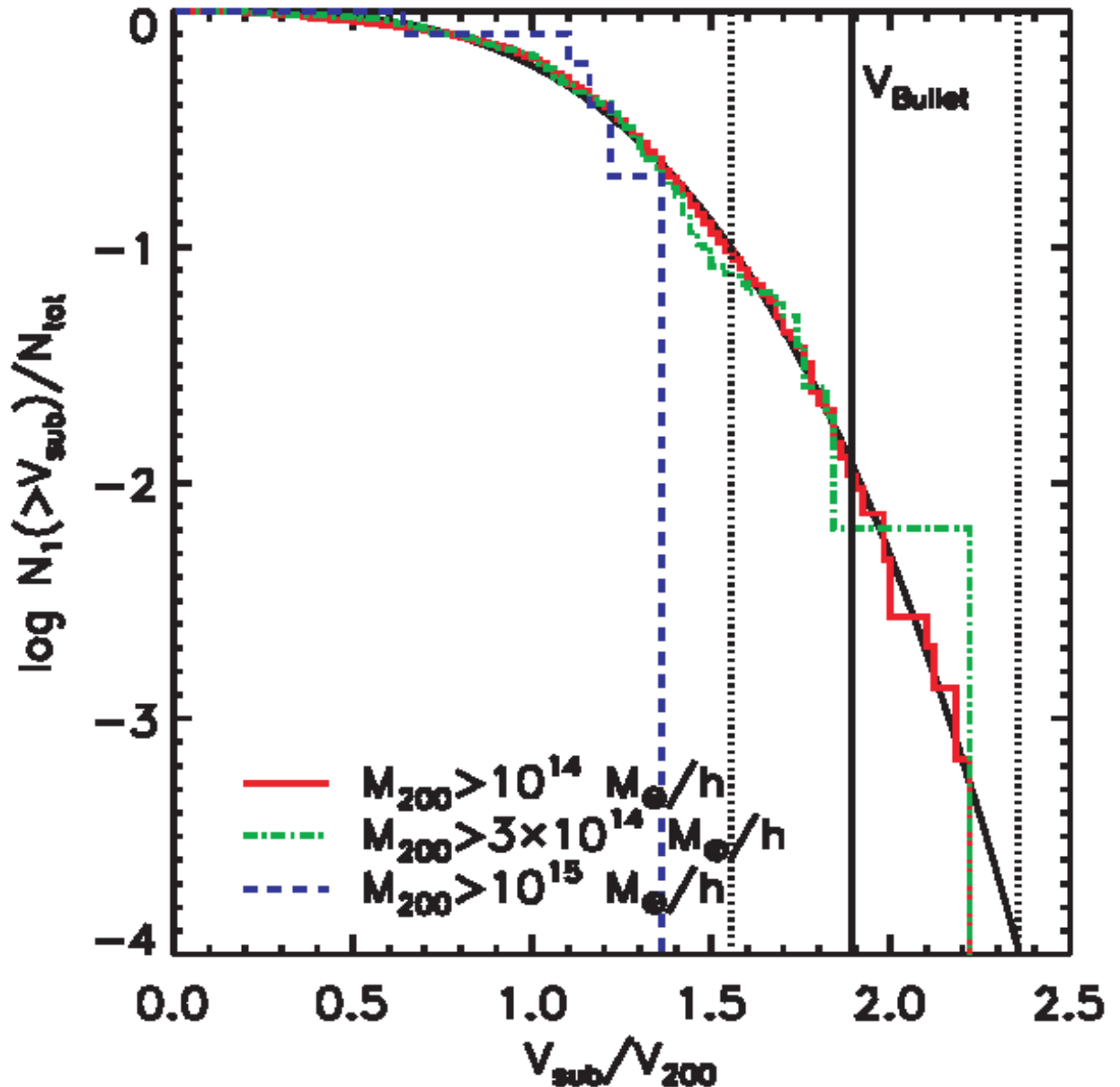
But, revised data from Clowe et al. (2006) and Markevitch et al. (2006):

$$M_{200} = 1.5 \times 10^{15} M_{\odot}$$

$$V_{200} = 1680 \text{ km/sec}$$

$$V_{\text{shock}} = 4740 \text{ km/sec}$$

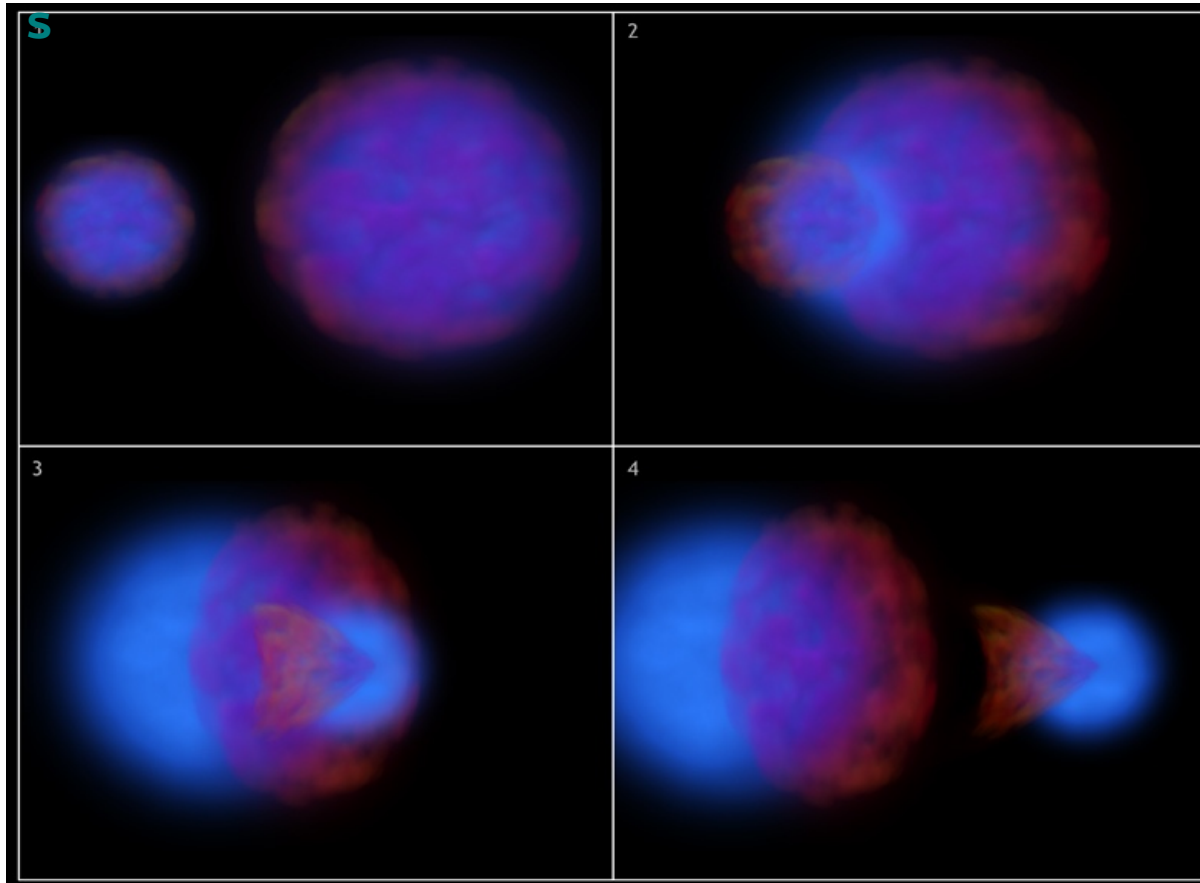
$$V_{\text{sub}}/V_{\text{shock}} = 2.8 \quad \text{chance: } 10^{-7}$$



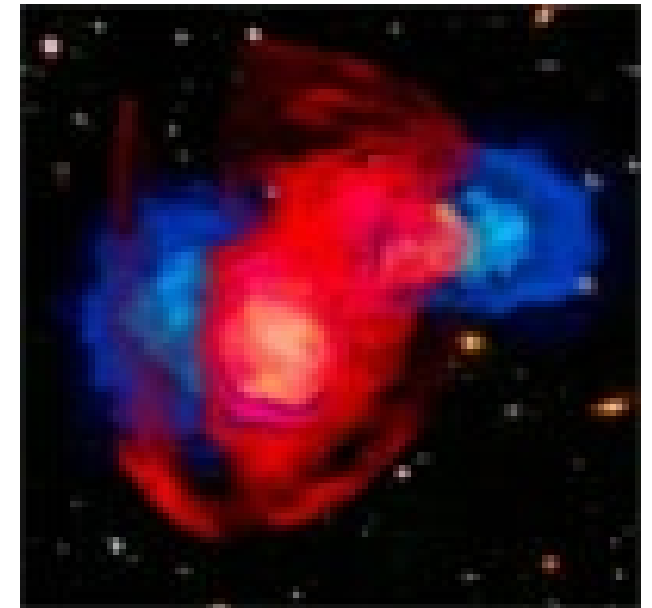
Simulating realistic models of the bullet cluster is key for a proper interpretation of the dynamical state of the system

### ANIMATIONS OF THE BULLET CLUSTER MERGER

NASA/CXC/M.Weis



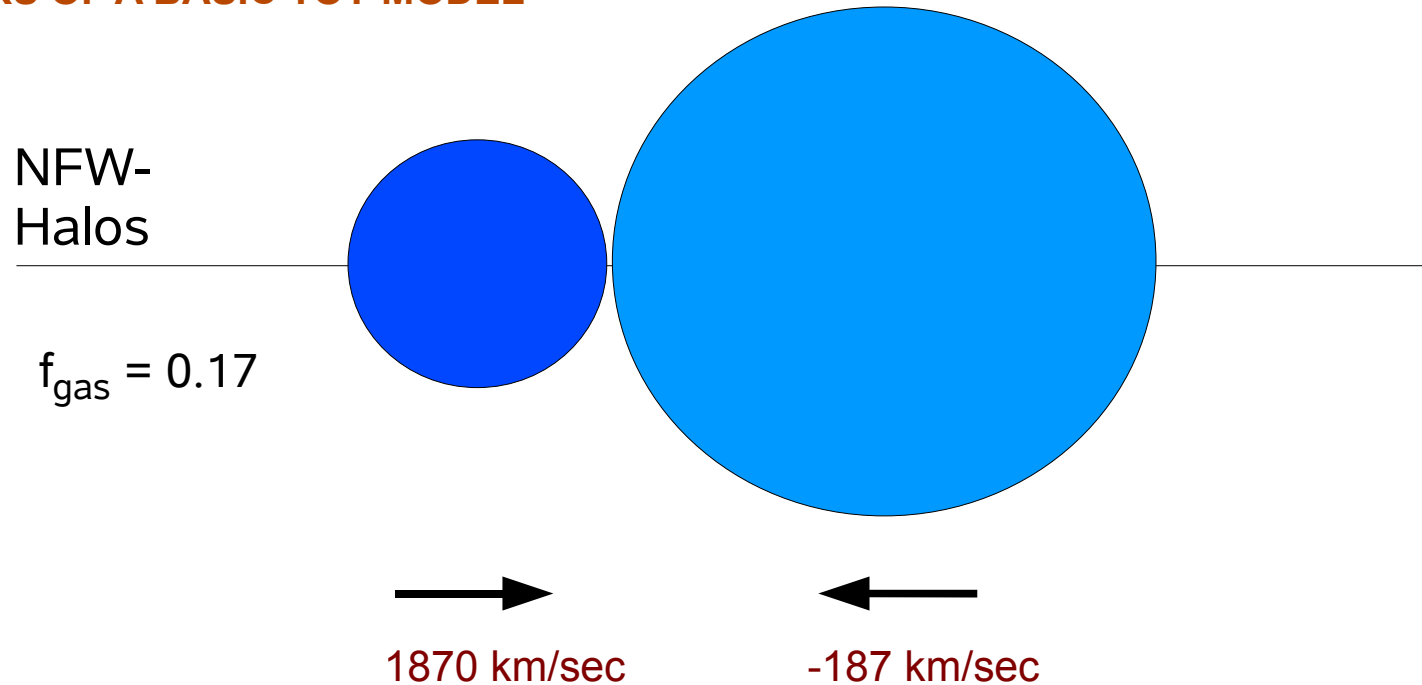
KIPAC/John Wise



(Note: The distance of the mass peaks is 720 kpc on the sky...)

# A simple toy merger model of two NFW halos on a zero-energy collision orbit

## PARAMETERS OF A BASIC TOY MODEL



## Mass model from Clowe et al. (2006):

$$M_{200} = 1.5 \times 10^{14} M_{\odot}$$

$$R_{200} = 1.1 \text{ Mpc}$$

$$c = 7.2$$

$$V_{200} = 780 \text{ km/sec}$$

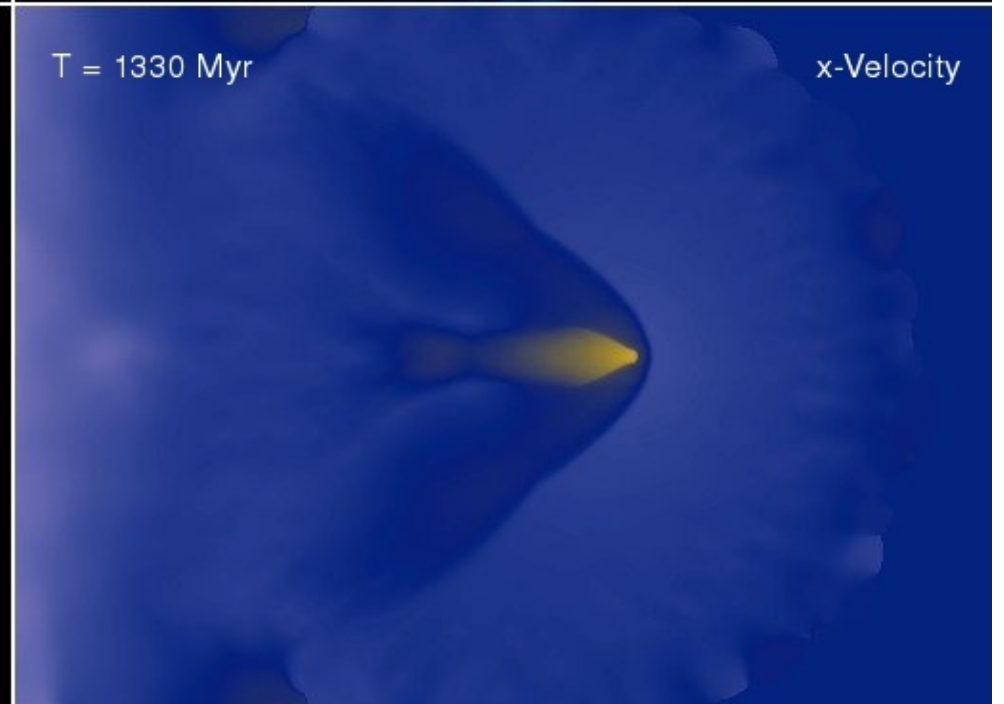
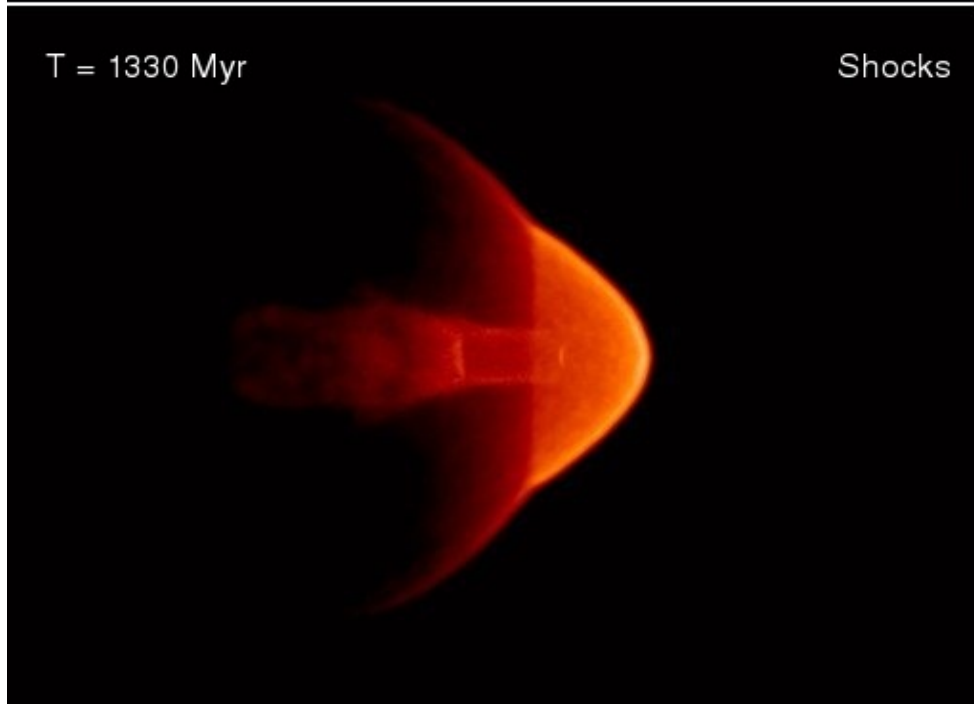
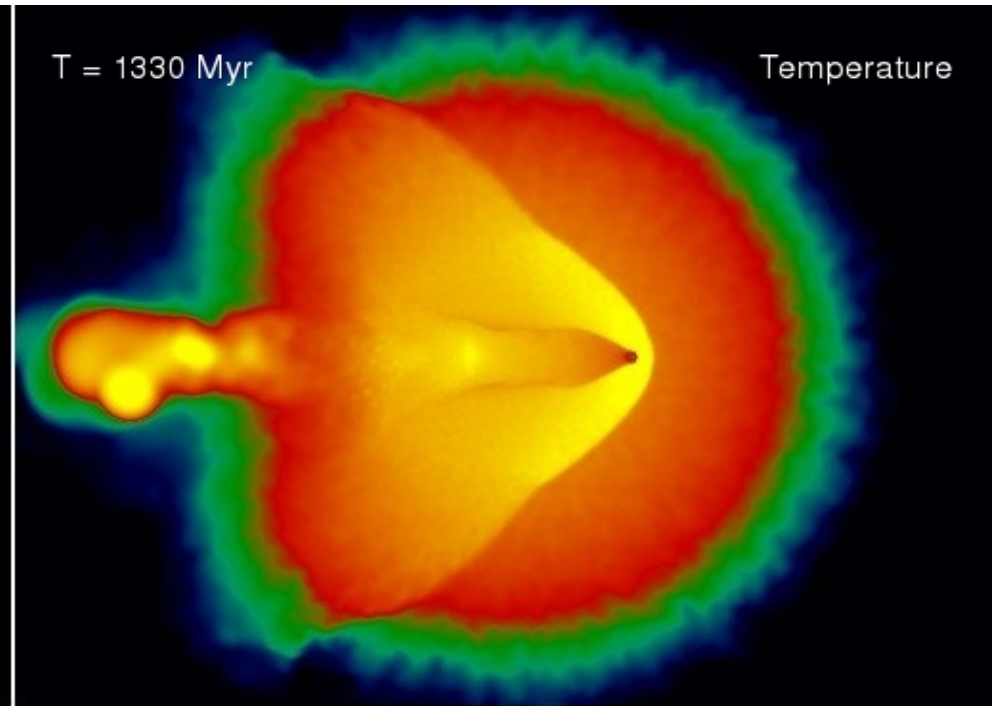
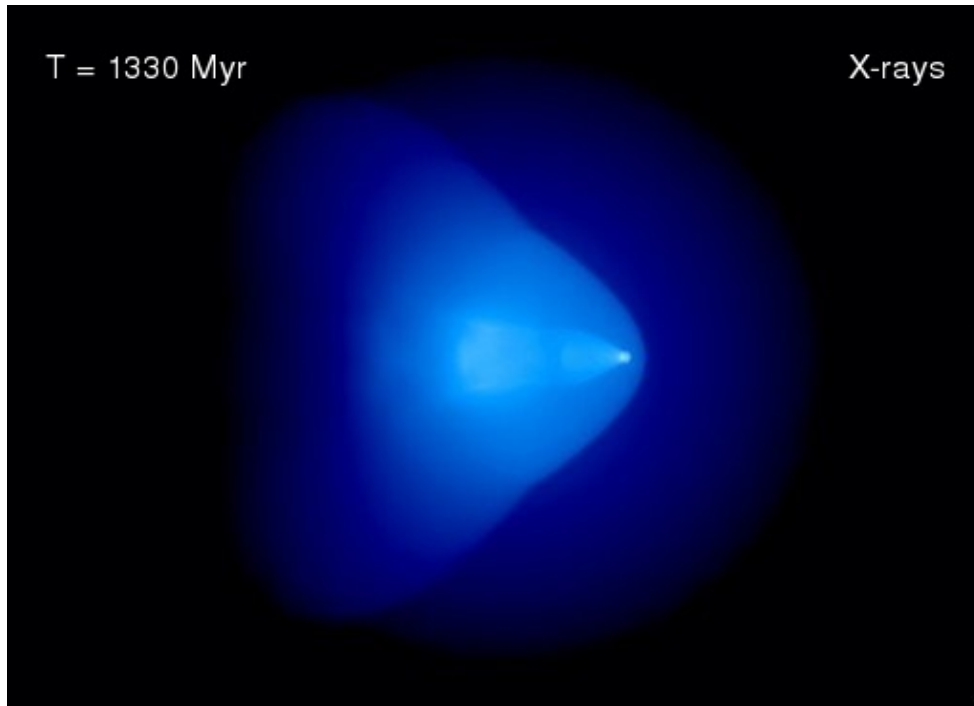
$$M_{200} = 1.5 \times 10^{15} M_{\odot}$$

$$R_{200} = 2.3 \text{ Mpc}$$

$$c = 2.0$$

$$V_{200} = 1680 \text{ km/sec}$$

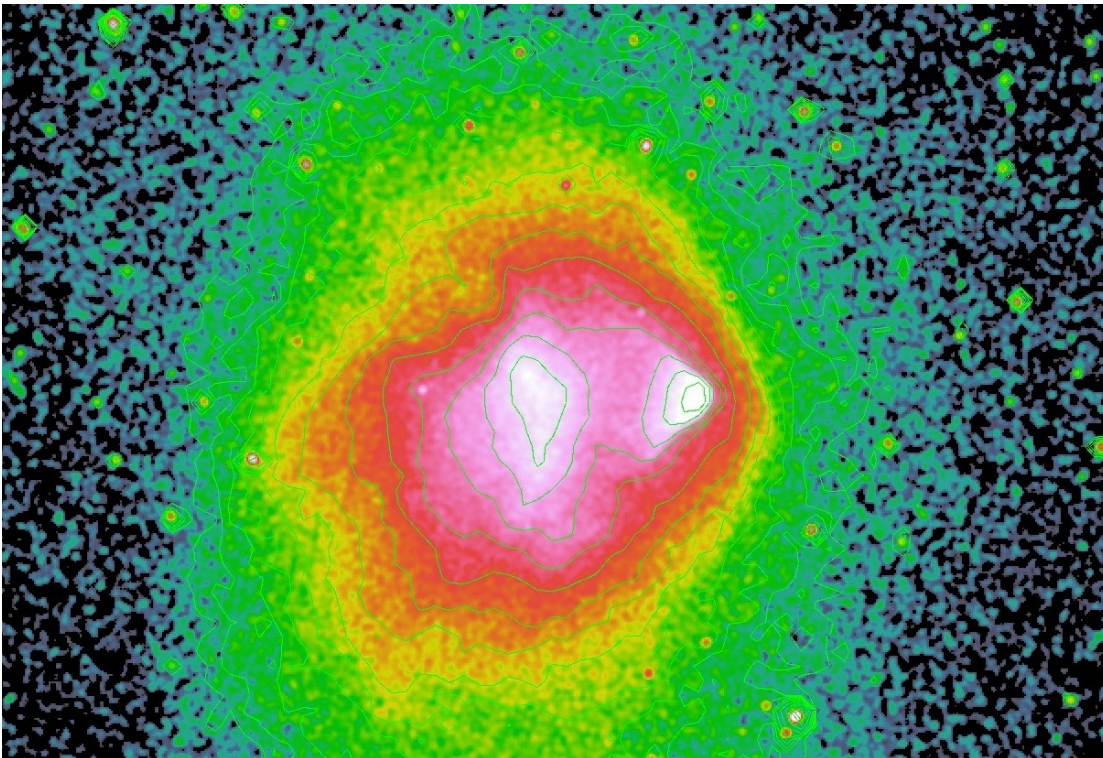
# VIDEO OF THE TIME EVOLUTION OF A SIMPLE BULLET CLUSTER MODEL



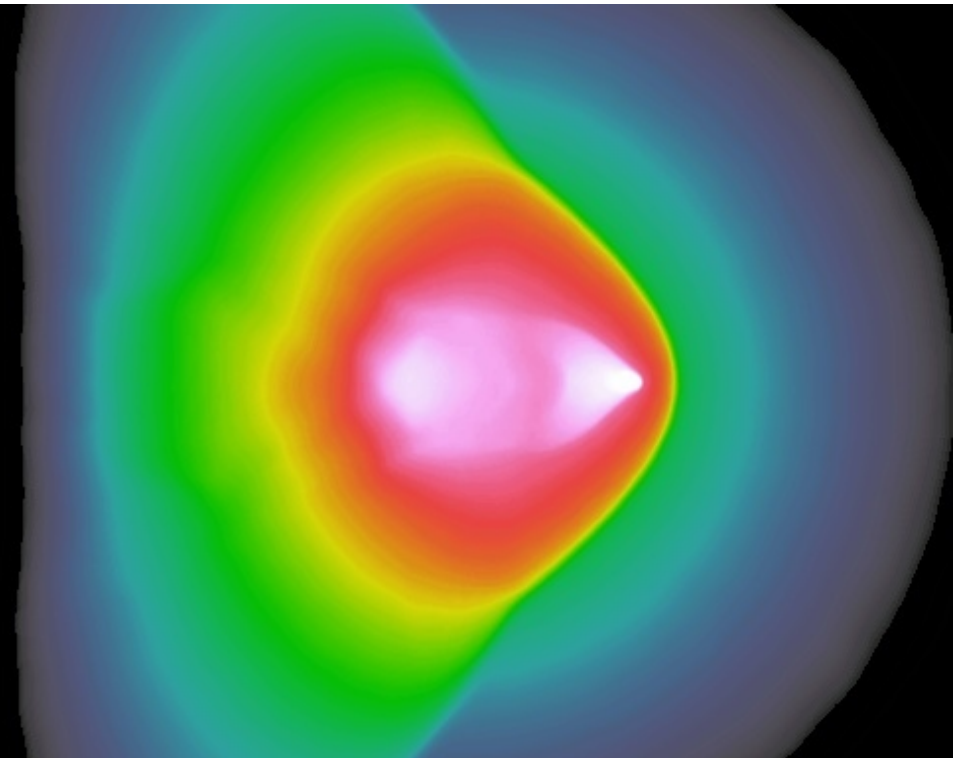
Drawing the observed X-ray map and the simulation images with the same color-scale simplifies the comparison

**SIMULATED X-RAY MAP COMPARED TO OBSERVATION**

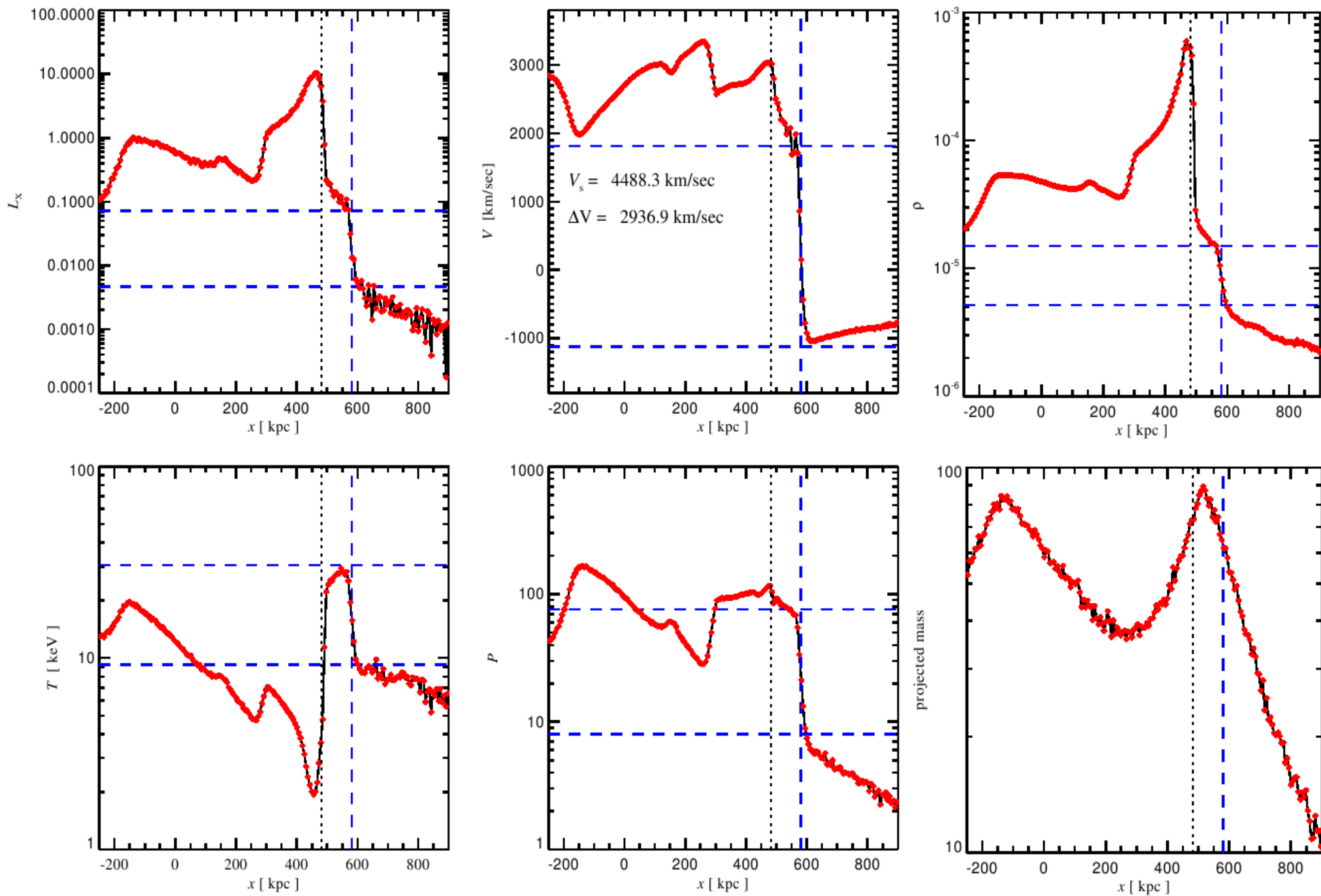
Candra 500 ks image



bullet cluster simulation

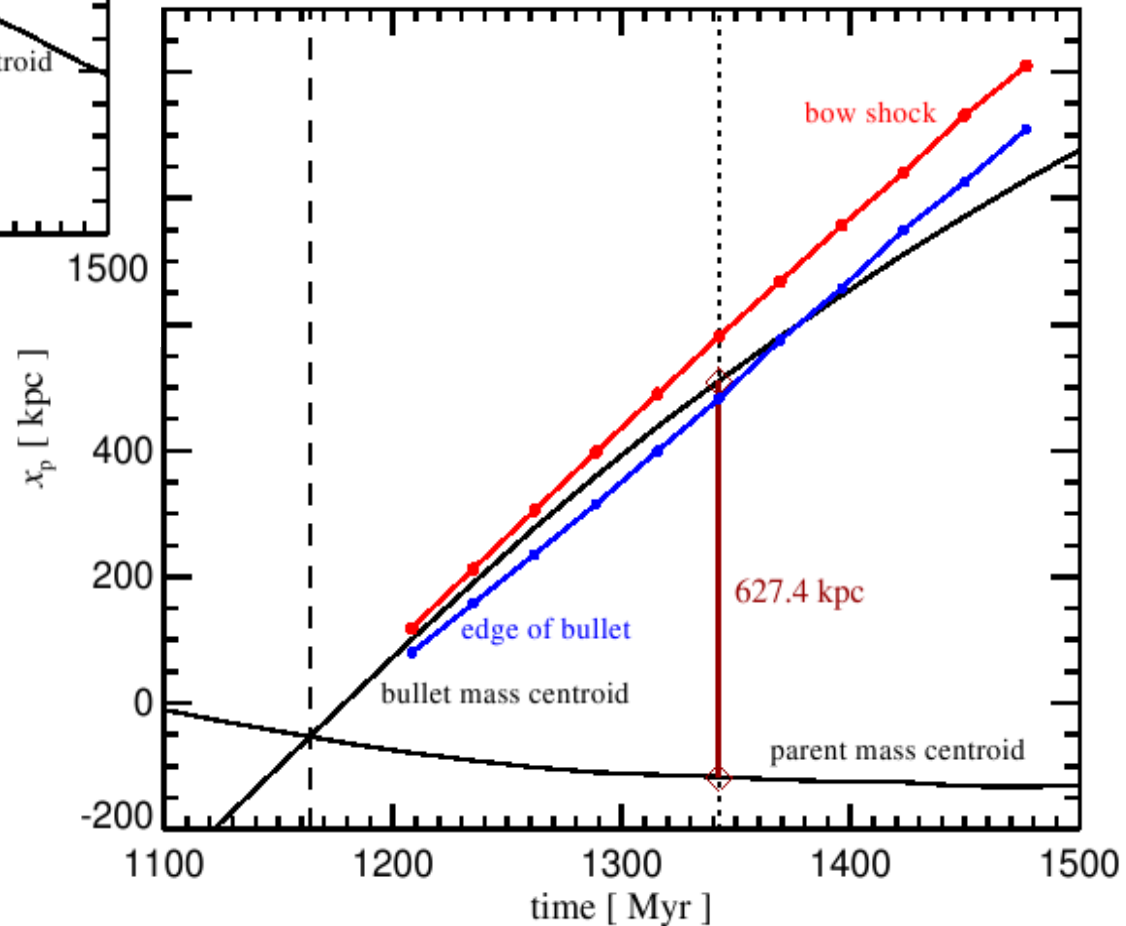
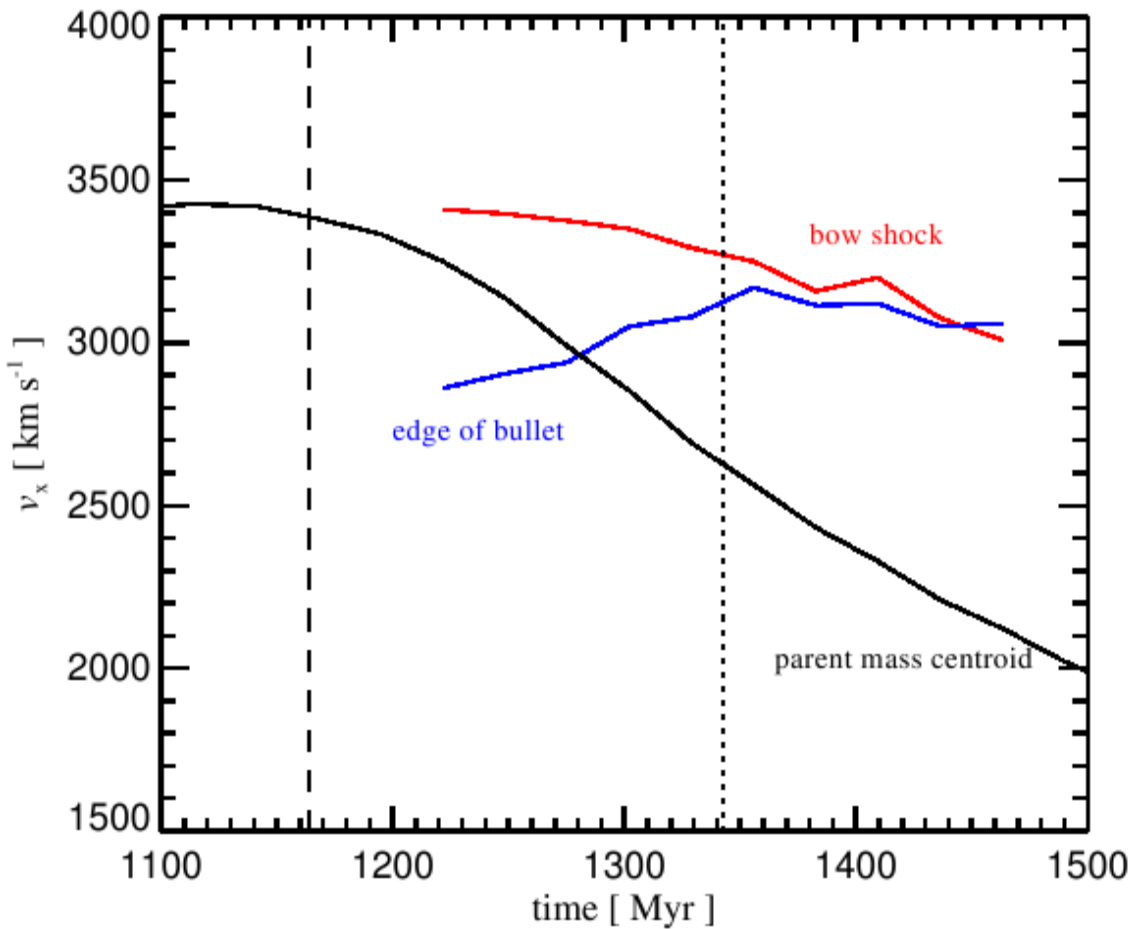


# Profiles along the collision axis reveal a strong shock and a cold front



Despite a shock speed of  $\sim 4500$  km/s, the bullet moves considerably slower

**VELOCITIES AND POSITIONS OF MAIN BULLET CLUSTER FEATURES AS A FUNCTION OF TIME**



Shock speed: 4500 km/s

Pre-shock infall: -1100 km/s

Shock speed  
relative to bullet: -800 km/s

**Speed of bullet: 2600 km/s**

The change of the potential can be used to estimate the energy gained by the dark matter particles in the parent cluster region ahead of the shock

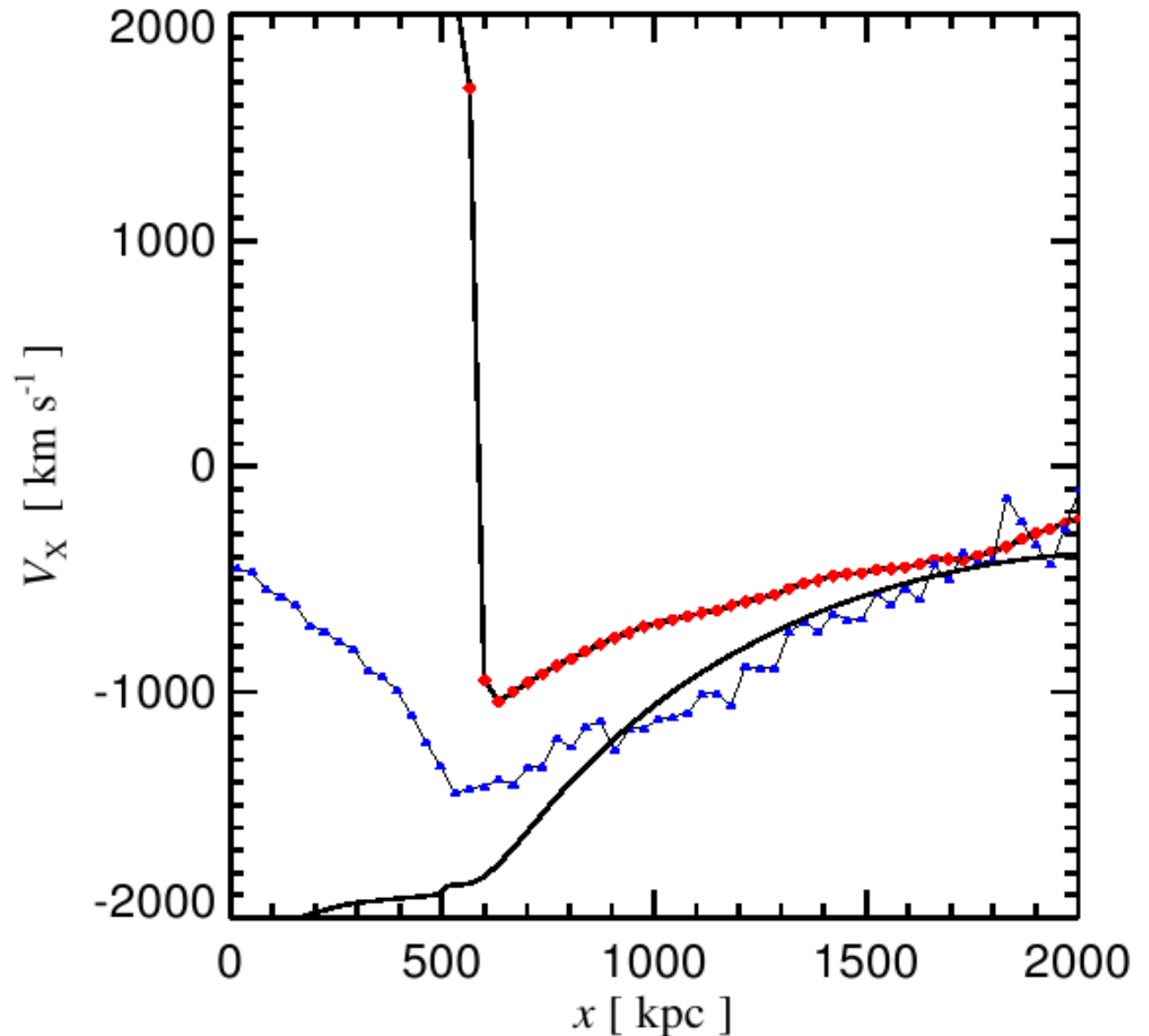
**ESTIMATE OF THE EXPECTED DARK MATTER STREAMING VELOCITY COMPARED TO THE SIMULATION**

$$e_i = v_i^2/2 + \Phi(\vec{x}_i)$$

$$de_i/dt = \partial\Phi/\partial t$$

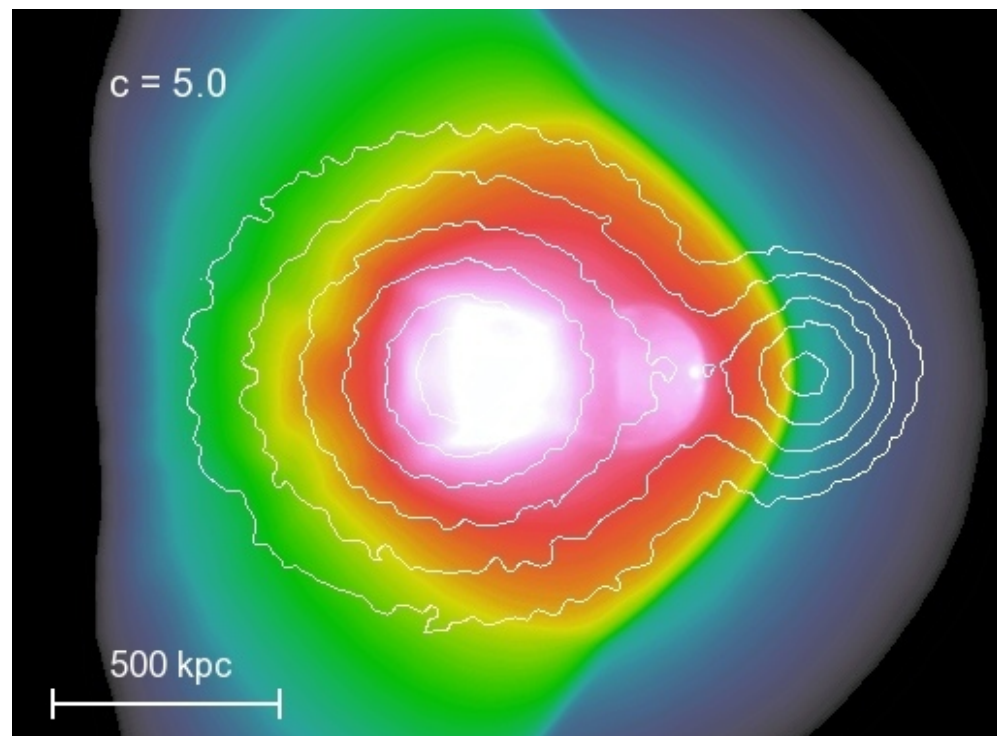
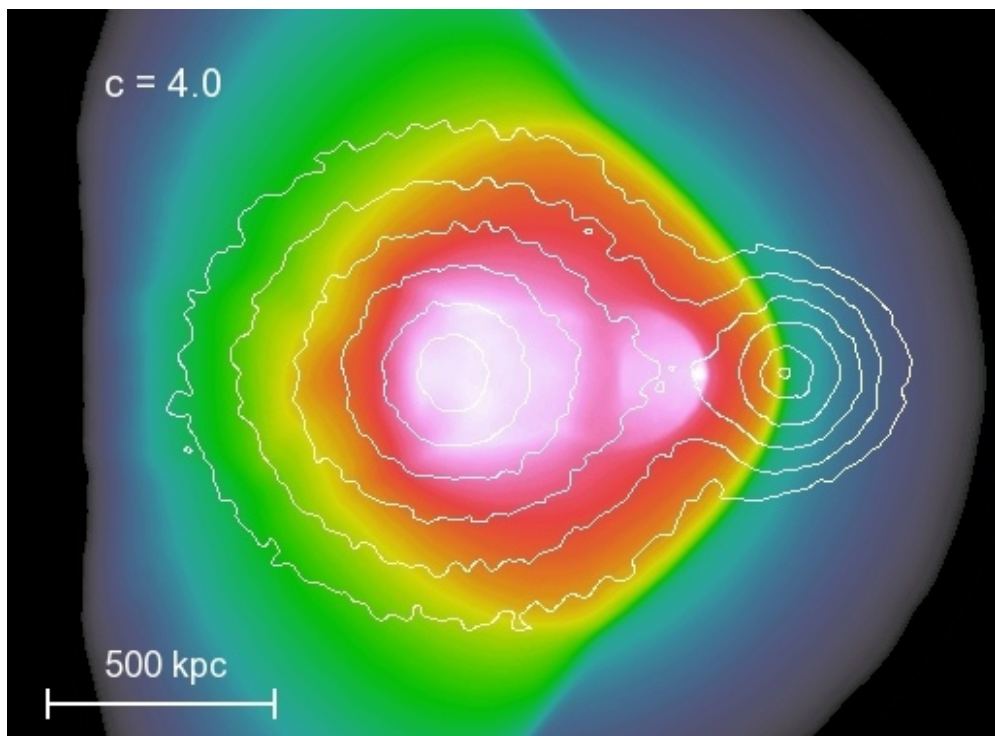
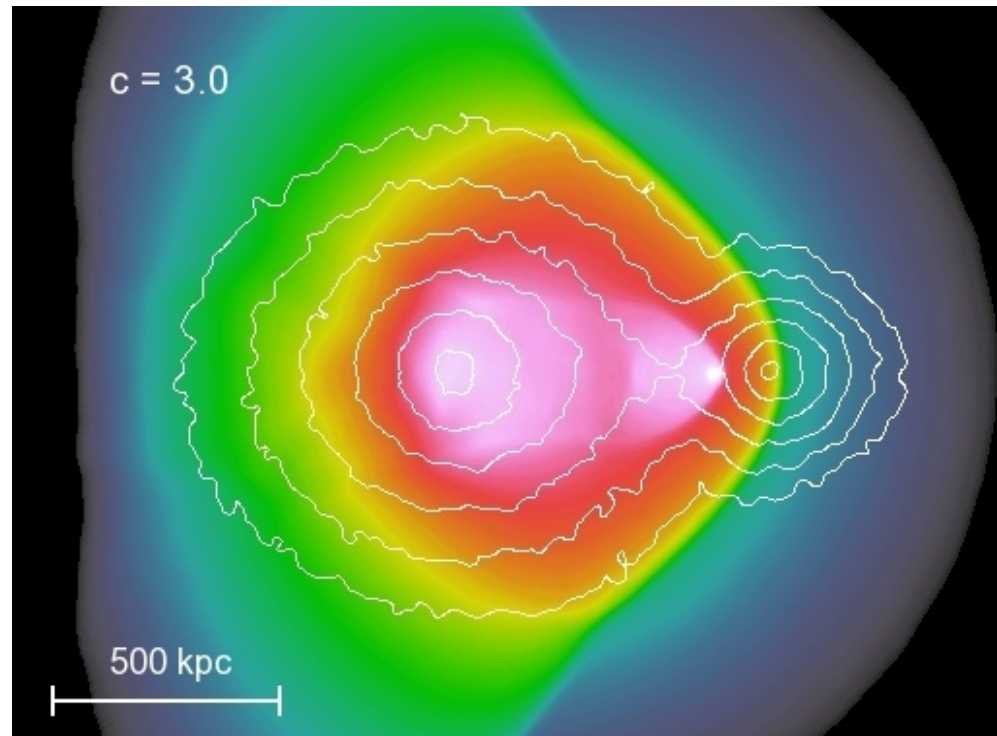
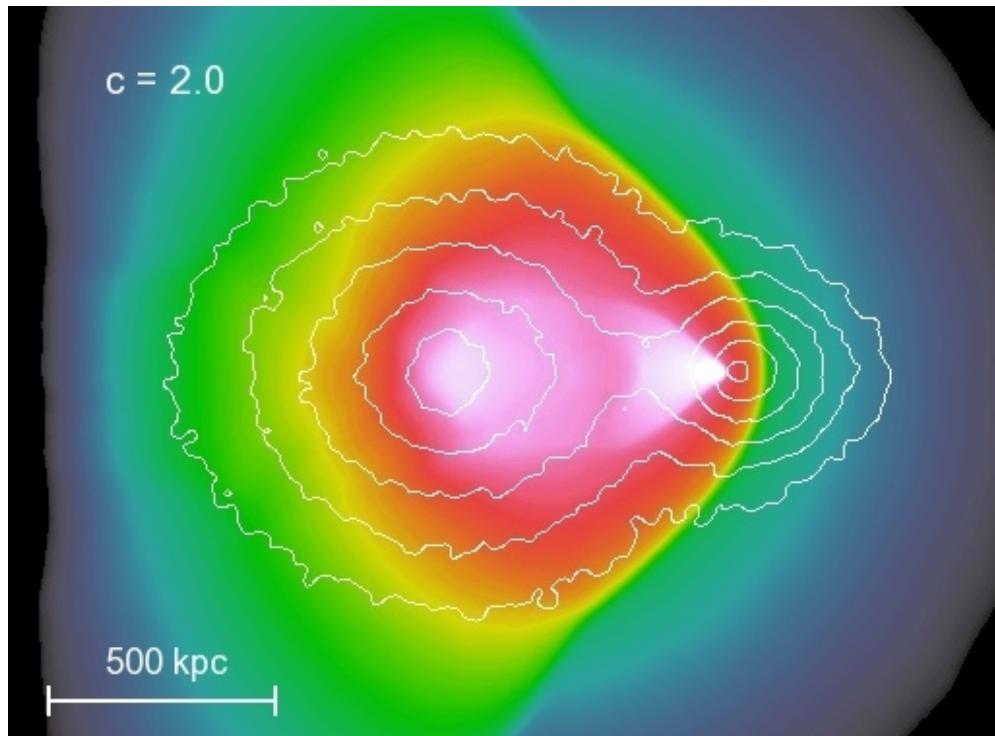


$$\tilde{v}_r^2 \simeq v_r^2 - 2\Delta\Phi$$



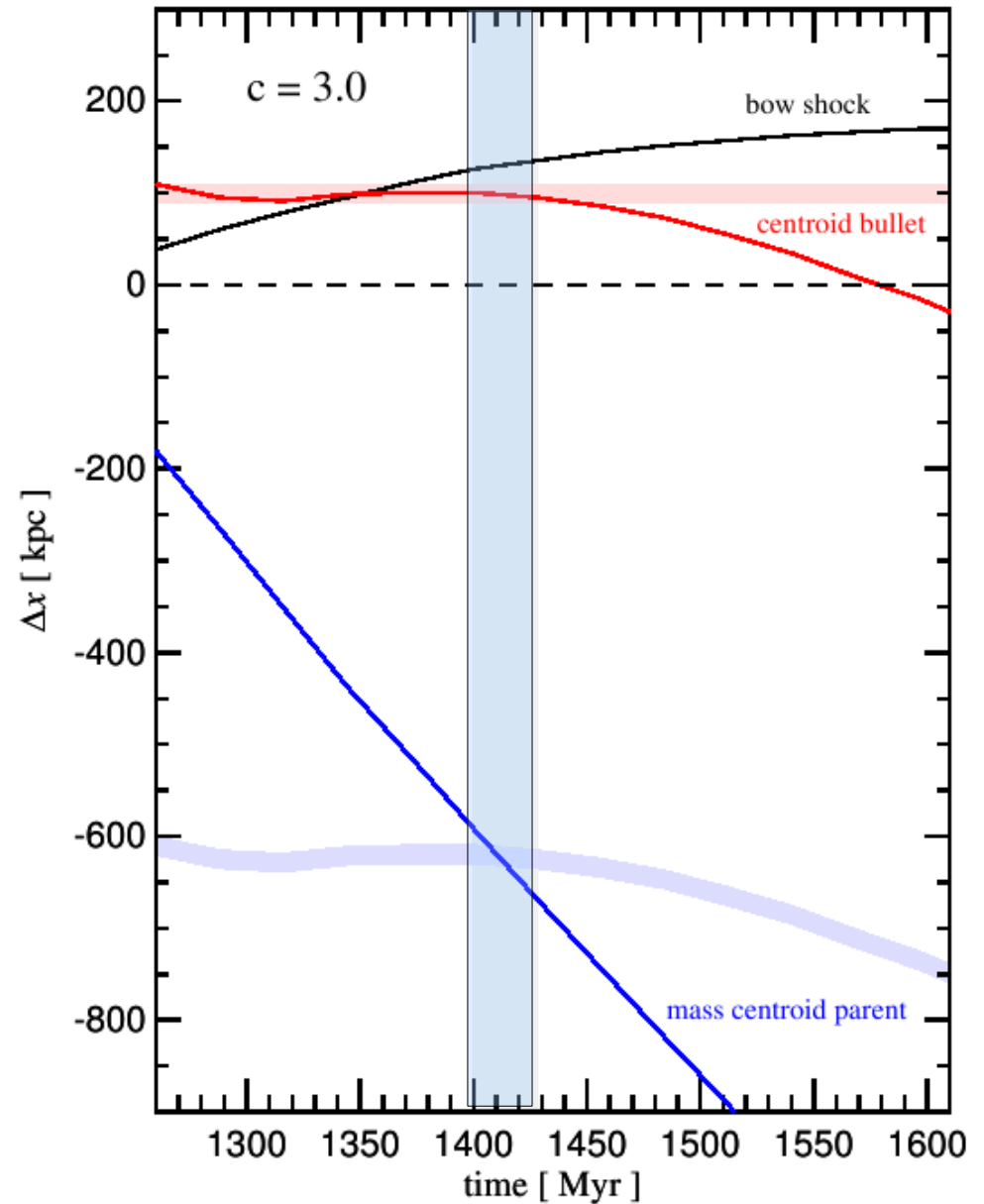
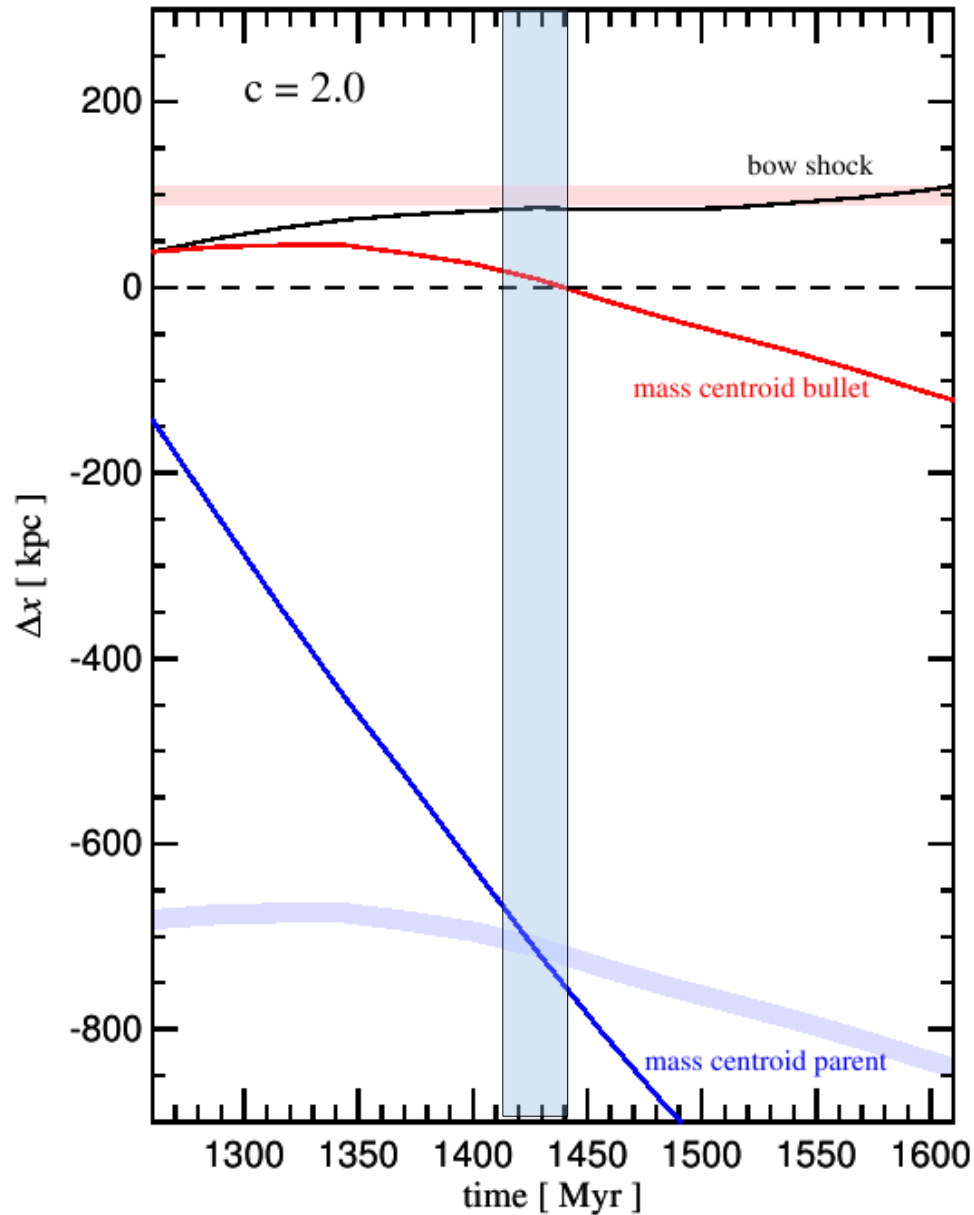


# Changing the structural properties of the parent cluster



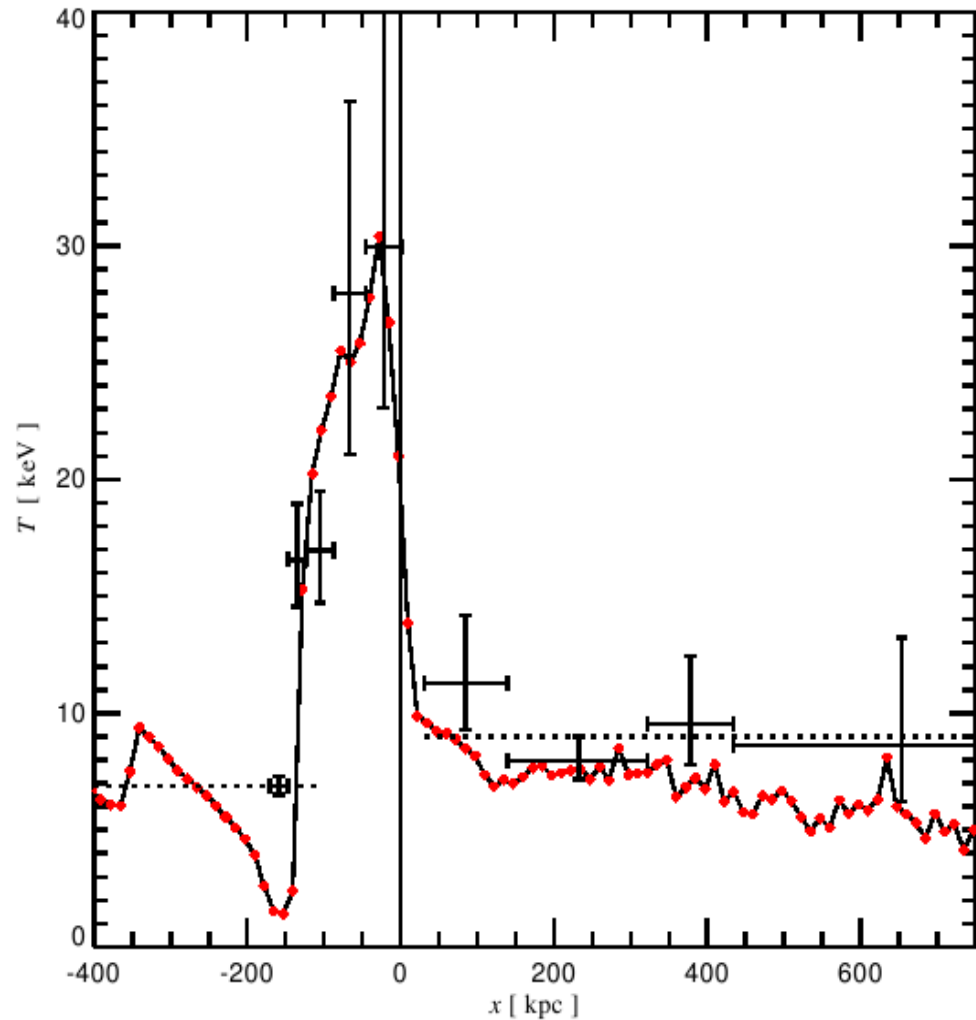
For  $c=3.0$  for the parent cluster, the model can simultaneously fit the cluster-bullet separation and the offset between the bullet's gas and mass peak

### SEPARATION OF FEATURES AS A FUNCTION OF TIME

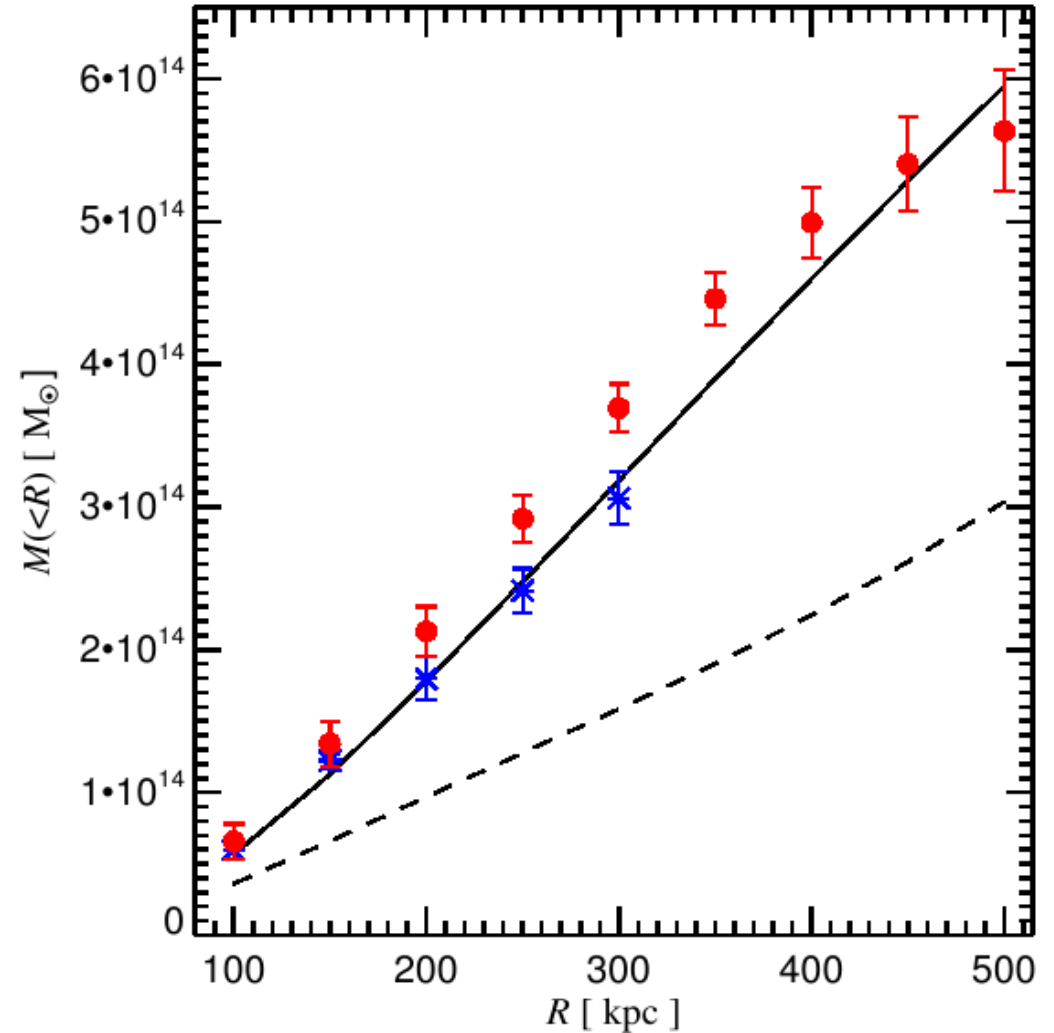


The model also matches the observed temperature and mass profiles

**COMPARISON OF SIMULATED TEMPERATURE AND MASS PROFILE WITH OBSERVATIONS**



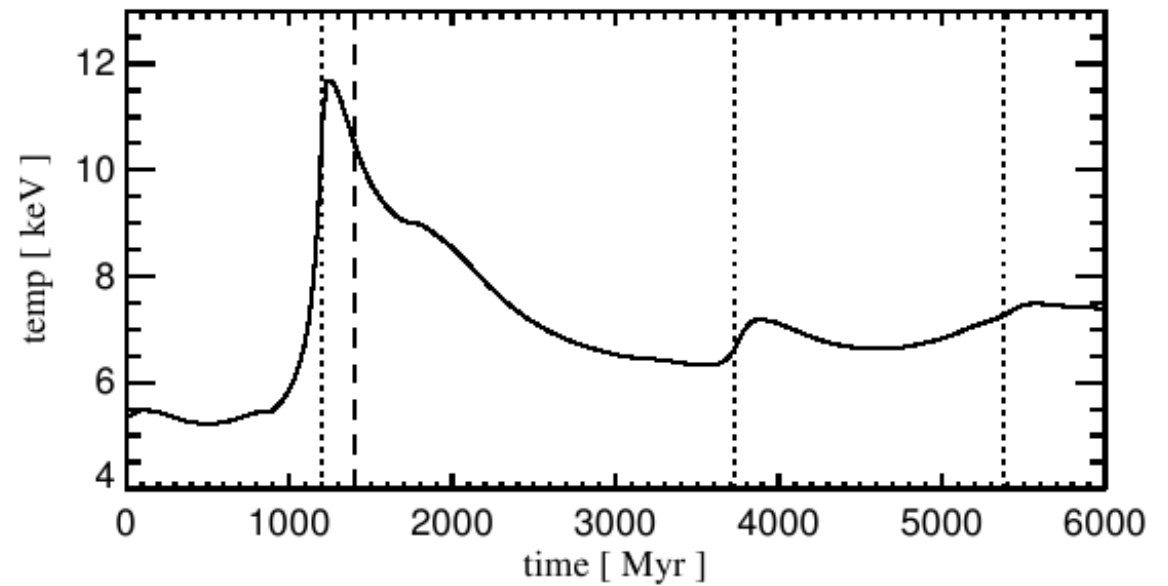
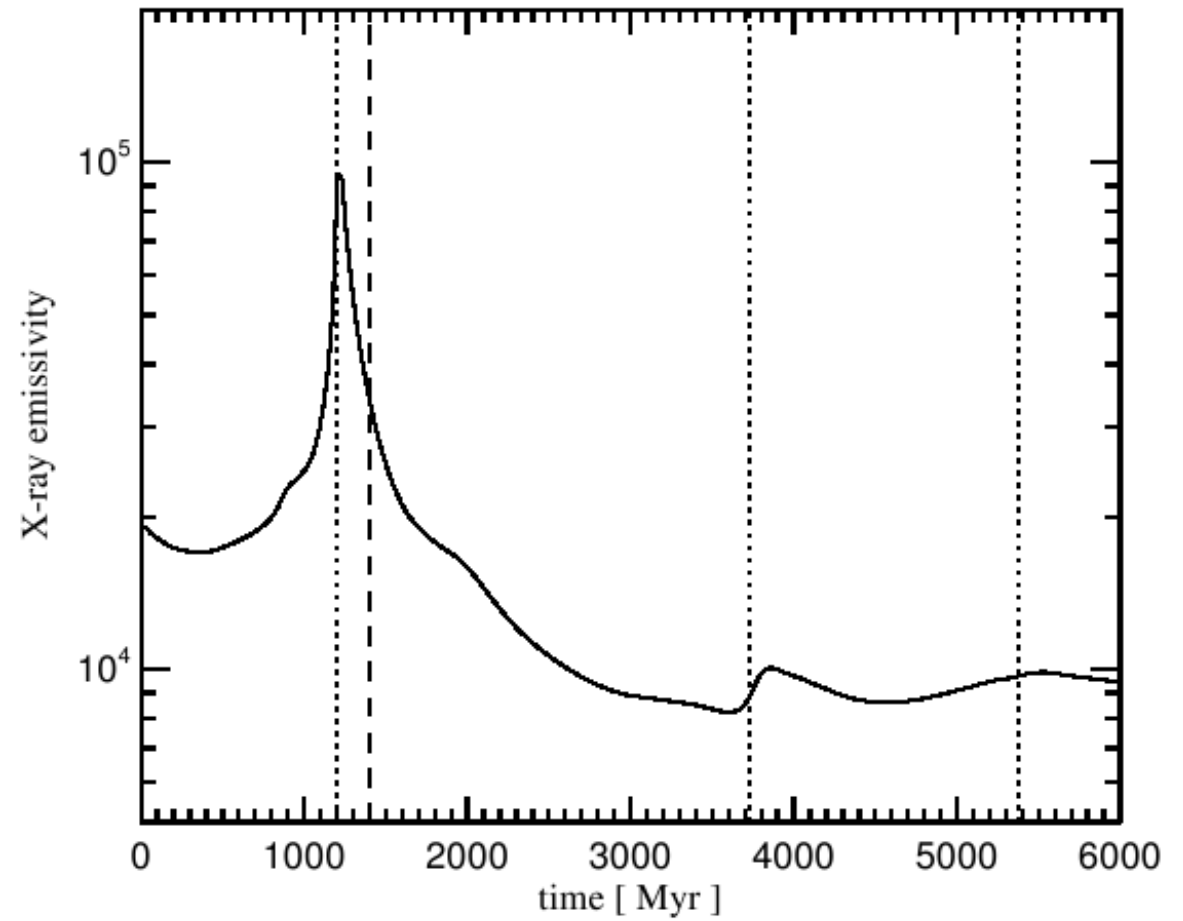
Data from Markevitch et al. (2006)



Data from Bradac et al. (2006)

The simulation model can be used to predict the future evolution of the bullet cluster

**TIME EVOLUTION OF X-RAY EMISSION AND X-RAY TEMPERATURE**



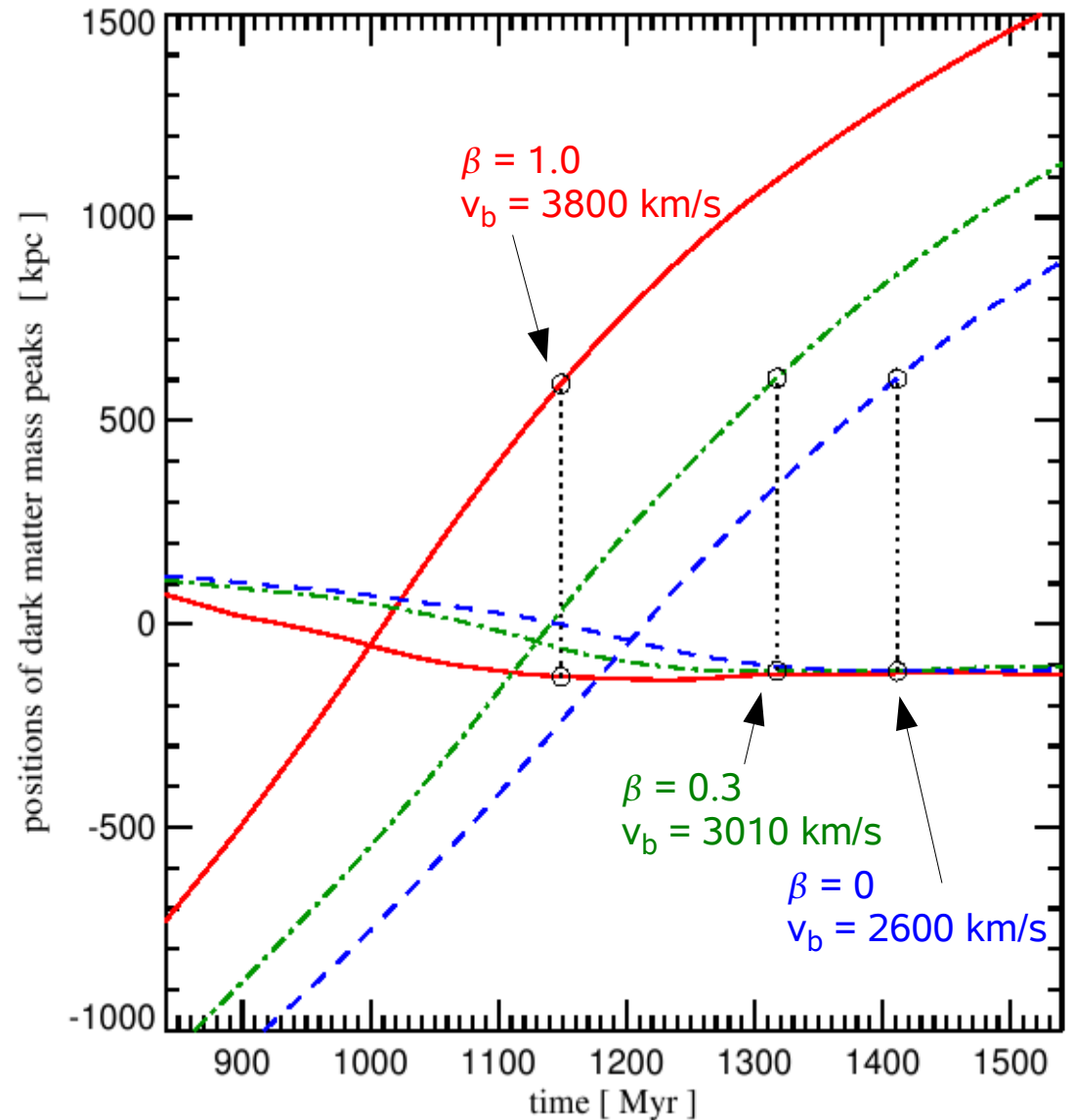
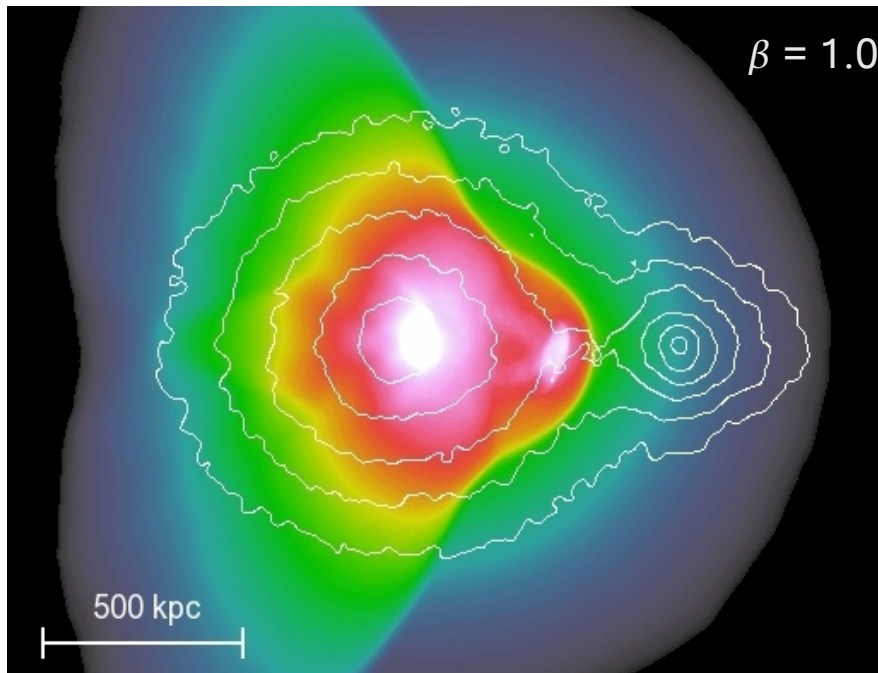
Models with a “fifth force” in the dark sector can speed up the bullet, but seem not required to match the bullet system

### SPEED OF THE BULLET IN FIFTH FORCE MERGERS

(proposed by Farrar & Rosen 2006)

$$\phi_s(r) = -\beta \frac{Gm}{r} \exp\left(-\frac{r}{r_s}\right)$$

- $\beta = 1.0$ ,  $r_s = 4$  Mpc
- $\beta = 0.3$ ,  $r_s = 4$  Mpc



# Examples for non- standard physics with SPH

# Thermal conduction may partially offset radiative cooling in central cluster regions

## THE CONDUCTION IDEA

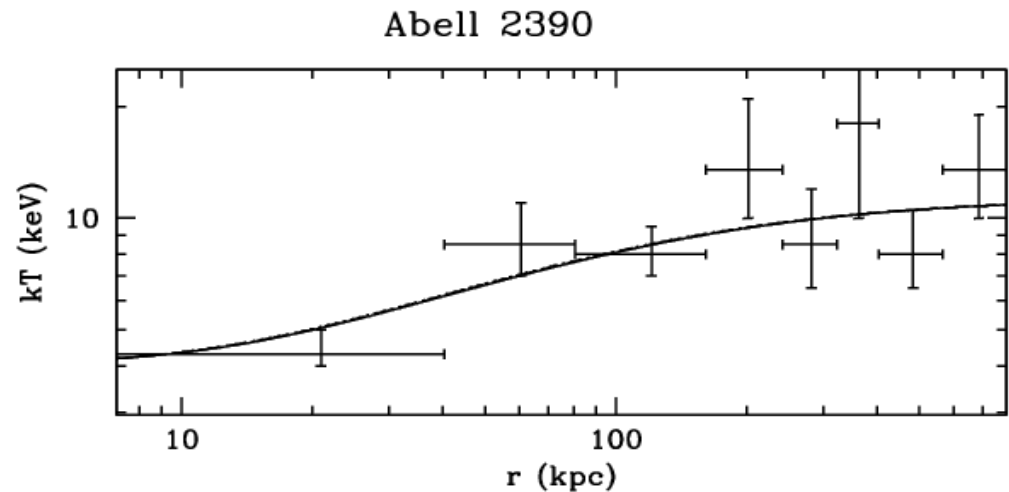
Inner region of clusters ( $\sim 10$ -50 kpc) is cooler than the rest of the cluster



Is thermal conduction from the outer hot regions of the cluster the heat source?

Zakamska & Narayan (2003)

- Assume hydrostatic equilibrium with a balance between cooling and conductive heating
- Temperature profiles of five clusters can be well fit, requiring conductivities of the order 30% Spitzer-value



**BUT:** Magnetic fields are the natural enemy of conduction....

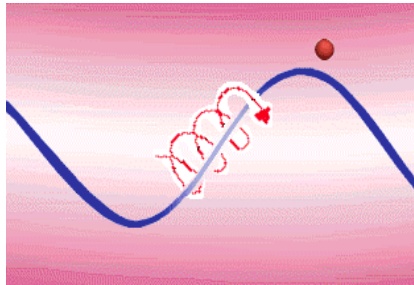
# Magnetic fields are the natural enemy of thermal conduction

## THE QUEST TO UNDERSTAND THE EFFECTIVE CONDUCTIVITY

Spitzer (1962) Conductivity of unmagnetized plasma:

$$\kappa_{\text{sp}} = 1.31 n_e \lambda_e k \left( \frac{kT_e}{m_e} \right)^{1/2} \quad \lambda_e n_e = \frac{3^{3/2} (kT_e)^2}{4\sqrt{\pi} e^4 \ln \Lambda}$$

→  $\kappa_{\text{sp}} \propto T_e^{5/2}$



If we have an ordered magnetic field:

$$\begin{aligned} \kappa_{\parallel} &\sim \kappa_{\text{sp}}/3 \\ \kappa_{\perp} &\sim (r_L/\lambda)^2 \kappa_{\text{sp}} \end{aligned}$$

In clusters:

$$\begin{aligned} B &\sim 10^{-6} \text{ G} \\ r_L &\sim 10^{-12} \lambda \end{aligned}$$

Rechester & Rosenbluth (1978)  
Chandran & Cowley (1998)  
Malyshkin & Kulsrud (2001)

If the field is **tangled**, the effective conductivity can be heavily suppressed:

$$\kappa_{\text{eff}} \sim \kappa_{\text{sp}}/100$$

Narayan & Medvedev (2001)

If the field is **chaotic on a range of turbulent scales**, conduction may almost reach the Spitzer value:

$$\kappa_{\text{turb}} \sim \kappa_{\text{sp}}/3$$



# A robust and accurate implementation of thermal conduction in SPH

## SPH DISCRETIZATION OF CONDUCTION

### Conduction equation:

$$\begin{aligned} \mathbf{j} &= -\kappa \nabla T & \frac{du}{dt} &= \frac{1}{\rho} \nabla (\kappa \nabla T) \\ \rho \frac{du}{dt} &= -\nabla \mathbf{j} \end{aligned}$$

Second-order derivative tends to be noisy...

### SPH discretization:

$$\frac{du_i}{dt} = \sum_j \frac{m_j}{\rho_i \rho_j} \frac{(\kappa_j + \kappa_i) (T_j - T_i)}{|\mathbf{x}_{ij}|^2} \mathbf{x}_{ij} \nabla_i W_{ij}$$

Brookshaw (1985)

### Problems encountered in practice:

- Explicit time integration can easily lead to instabilities
- Individual timestepping may easily lead to errors in energy conservation (conductivity depends strongly on temperature)

—————▶ Best solved with implicit **time integration** schemes, which guarantee robustness

# Derivation of the Laplace operator in SPH

Start with a Taylor expansion to third order

$$Y(\mathbf{x}_j) - Y(\mathbf{x}_i) = \nabla Y \Big|_{\mathbf{x}_i} \cdot (\mathbf{x}_j - \mathbf{x}_i) + \frac{1}{2} \frac{\partial^2 Y}{\partial x_s \partial x_k} \Big|_{\mathbf{x}_i} (\mathbf{x}_j - \mathbf{x}_i)_s (\mathbf{x}_j - \mathbf{x}_i)_k + \mathcal{O}(\mathbf{x}_j - \mathbf{x}_i)^3$$

We multiply through with the factor  $\frac{(\mathbf{x}_j - \mathbf{x}_i) \nabla_i W(\mathbf{x}_j - \mathbf{x}_i)}{|\mathbf{x}_j - \mathbf{x}_i|^2}$  and integrate over space.

Noting that

$$\int \mathbf{x}_{ij} \frac{\mathbf{x}_{ij} \nabla_i W_{ij}}{|\mathbf{x}_{ij}|^2} d^3 \mathbf{x}_j = 0, \quad \int (\mathbf{x}_{ij})_s (\mathbf{x}_{ij})_k \frac{\mathbf{x}_{ij} \nabla_i W_{ij}}{|\mathbf{x}_{ij}|^2} d^3 \mathbf{x}_j = \delta_{sk}$$

we arrive at

$$\nabla^2 Y \Big|_{\mathbf{x}_i} = -2 \int \frac{Y(\mathbf{x}_j) - Y(\mathbf{x}_i)}{|\mathbf{x}_{ij}|^2} \mathbf{x}_{ij} \nabla_i W_{ij} d^3 \mathbf{x}_j$$

Finally, change integration to SPH sum:

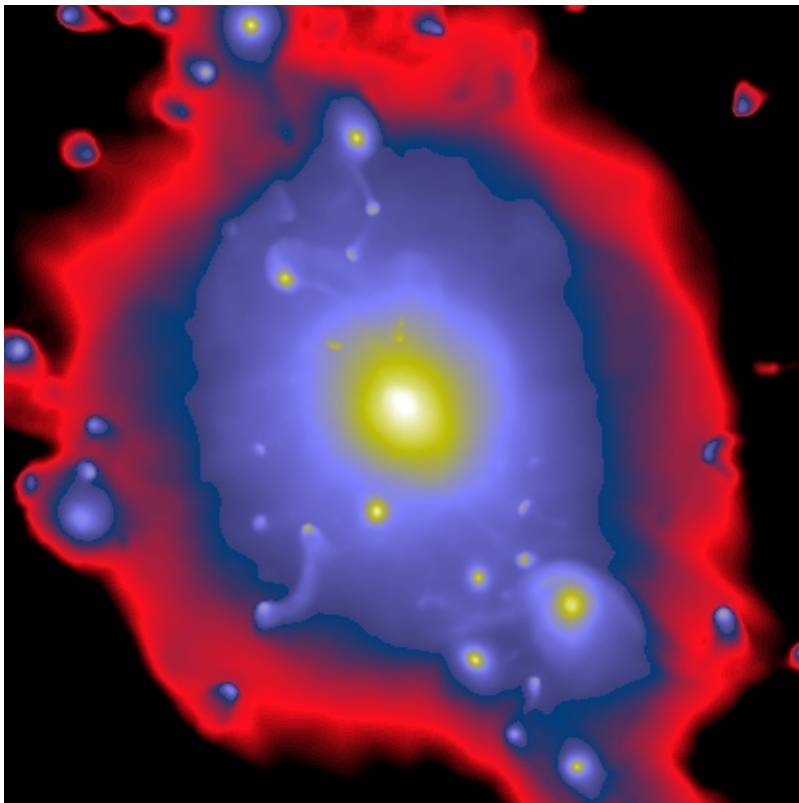
$$\nabla^2 Y \Big|_i = -2 \sum_j \frac{m_j}{\rho_j} \frac{Y_j - Y_i}{|\mathbf{x}_{ij}|^2} \mathbf{x}_{ij} \nabla_i W_{ij}$$

Self-consistent cosmological simulations of cluster formation can be used to study the impact of conduction on the ICM

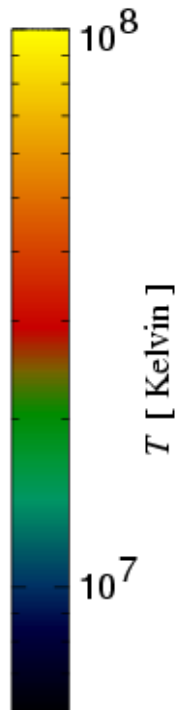
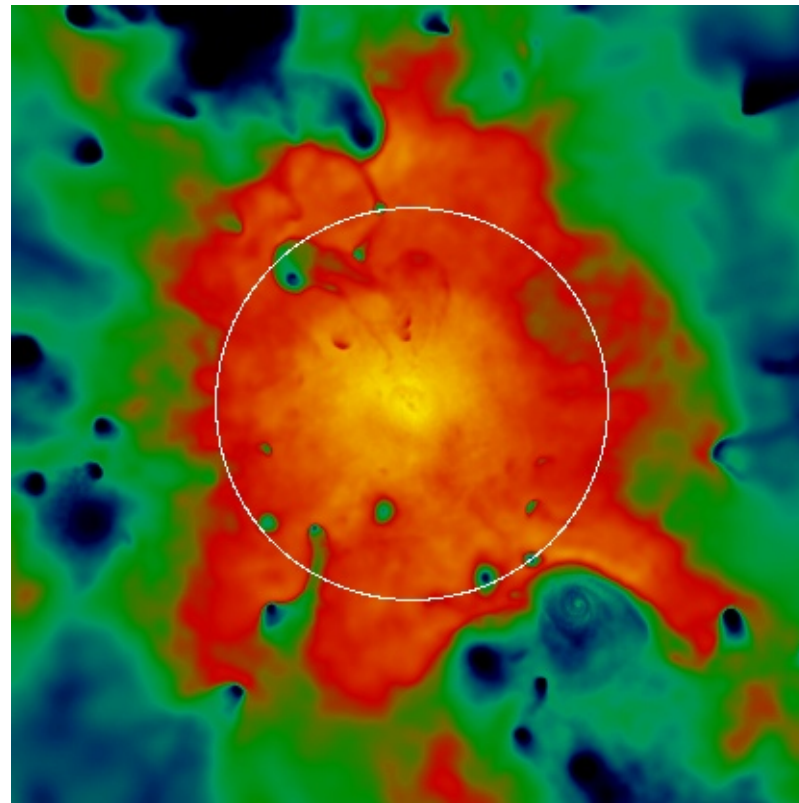
## X-RAY AND TEMPERATURE MAPS

Coma-sized cluster,  $M_{\text{vir}} \sim 10^{15} M_{\odot}$ , adiabatic hydrodynamics

Gas density (X-rays)



Mass-weighted temperature

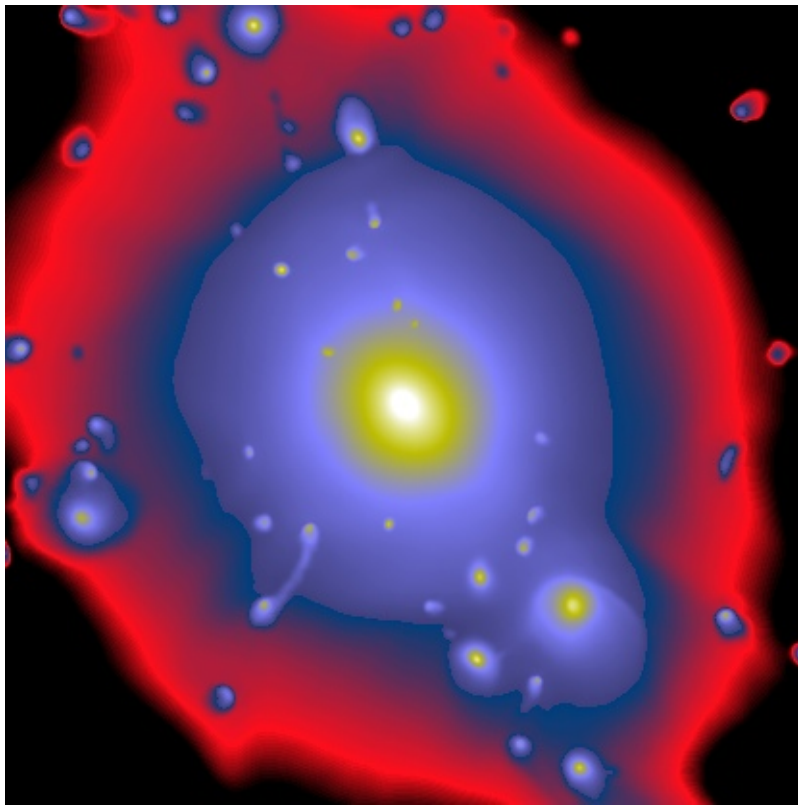


# Thermal conduction near the Spitzer value strongly affects rich clusters of galaxies

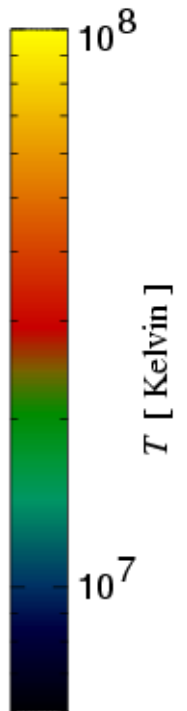
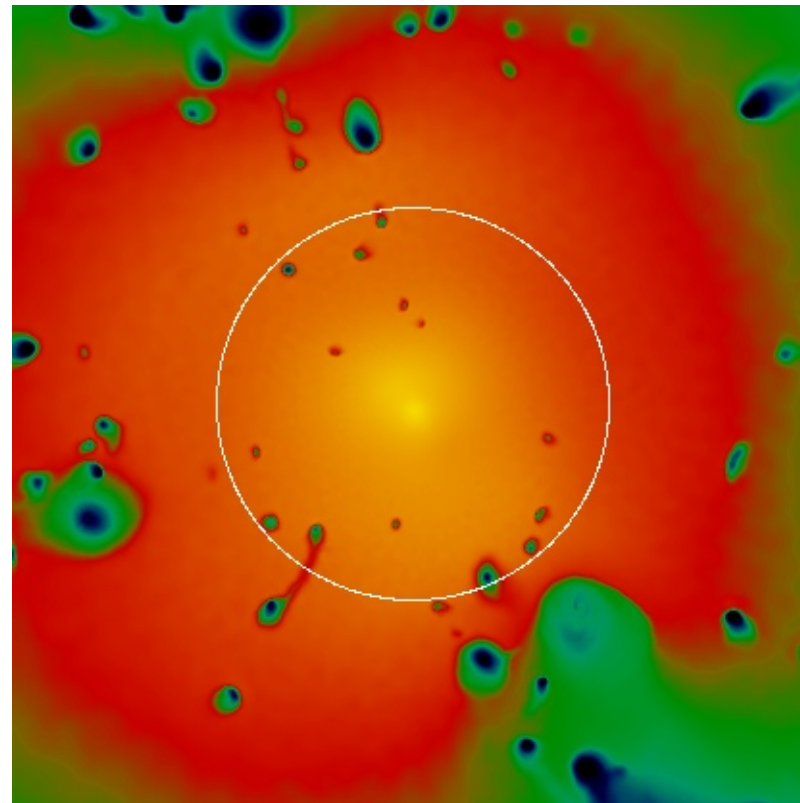
## X-RAY AND TEMPERATURE MAPS

Coma-sized cluster,  $M_{\text{vir}} \sim 10^{15} M_{\odot}$ ,  
adiabatic hydrodynamics, **thermal conduction with  $\kappa = \kappa_{\text{sp}}$**

Gas density (X-rays)



Mass-weighted temperature



# Physical viscosity in SPH

One can also derive an SPH discretization of the Navier-Stokes equations

## SPH WITH PHYSICAL VISCOUS STRESSES

Viscous stresses modify the momentum flux density tensor:  $\Pi_{ik} = p\delta_{ik} + \rho v_i v_k - \sigma_{ik}$

The stress tensor can be written as:

$$\sigma_{ik} = \eta \left( \frac{\partial v_i}{\partial x_k} + \frac{\partial v_k}{\partial x_i} - \frac{2}{3} \delta_{ik} \frac{\partial v_l}{\partial x_l} \right) + \zeta \delta_{ik} \frac{\partial v_l}{\partial x_l}$$

Shear viscosity coefficient

Bulk viscosity coefficient

The Euler equation of ideal gas dynamics is then replaced by the **Navier Stokes equations:**

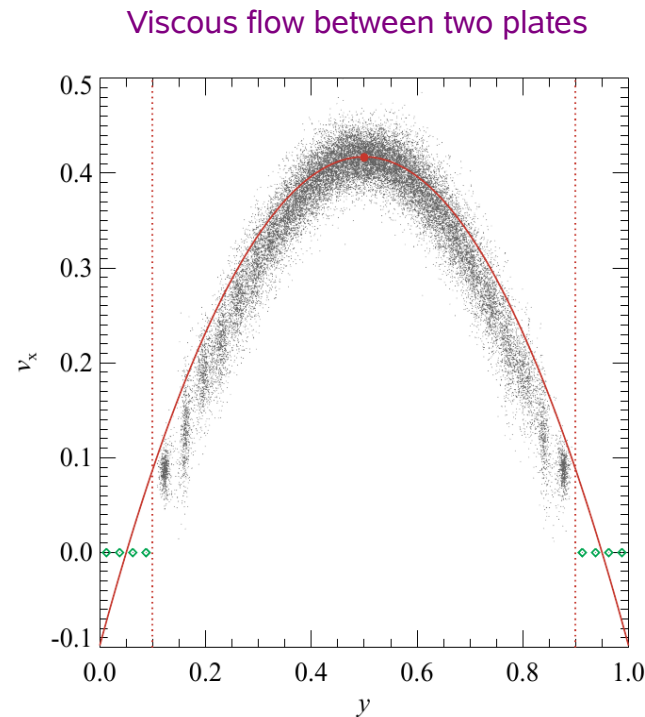
$$\begin{aligned} \rho \left( \frac{\partial v_i}{\partial t} + v_k \frac{\partial v_i}{\partial x_k} \right) = & -\frac{\partial p}{\partial x_i} - \rho \frac{\partial \Phi}{\partial x_i} \\ & + \frac{\partial}{\partial x_k} \left[ \eta \left( \frac{\partial v_i}{\partial x_k} + \frac{\partial v_k}{\partial x_i} - \frac{2}{3} \delta_{ik} \frac{\partial v_l}{\partial x_l} \right) \right] \\ & + \frac{\partial}{\partial x_i} \left( \zeta \frac{\partial v_l}{\partial x_l} \right) \end{aligned}$$

If conduction is also included, the thermal energy equation becomes the **generalized heat transfer equation:**

$$\rho T \frac{dS}{dt} = \nabla(\kappa \nabla T) + \frac{1}{2} \eta \sigma_{\alpha\beta} \sigma_{\alpha\beta} + \zeta (\nabla v)^2$$

# SPH discretization of the Navier-Stokes equations

## SPH WITH PHYSICAL VISCOUS STRESSES



$$\left. \frac{\partial v_\alpha}{\partial x_\beta} \right|_i = \frac{1}{\rho_i} \sum_{j=1}^N m_j (\mathbf{v}_j - \mathbf{v}_i)_\alpha [\nabla_i W_{ij}(h_i)]_\beta$$

$$\sigma_{\alpha\beta} \Big|_i = \eta \left( \left. \frac{\partial v_\alpha}{\partial x_\beta} \right|_i + \left. \frac{\partial v_\beta}{\partial x_\alpha} \right|_i - \frac{2}{3} \delta_{\alpha\beta} \left. \frac{\partial v_\gamma}{\partial x_\gamma} \right|_i \right) + \zeta \delta_{\alpha\beta} \left. \frac{\partial v_\gamma}{\partial x_\gamma} \right|_i$$

$$\left. \frac{dv_\alpha}{dt} \right|_{i,\text{shear}} = \sum_{j=1}^N m_j \left[ \frac{\eta_i \sigma_{\alpha\beta} \Big|_i}{\rho_i^2} [\nabla_i W_{ij}(h_i)]_\beta + \frac{\eta_j \sigma_{\alpha\beta} \Big|_j}{\rho_j^2} [\nabla_i W_{ij}(h_j)]_\beta \right]$$

$$\left. \frac{d\mathbf{v}}{dt} \right|_{i,\text{bulk}} = \sum_{j=1}^N m_j \left[ \frac{\zeta_i \nabla \cdot \mathbf{v}_i}{\rho_i^2} \nabla_i W_{ij}(h_i) + \frac{\zeta_j \nabla \cdot \mathbf{v}_j}{\rho_j^2} \nabla_i W_{ij}(h_j) \right]$$

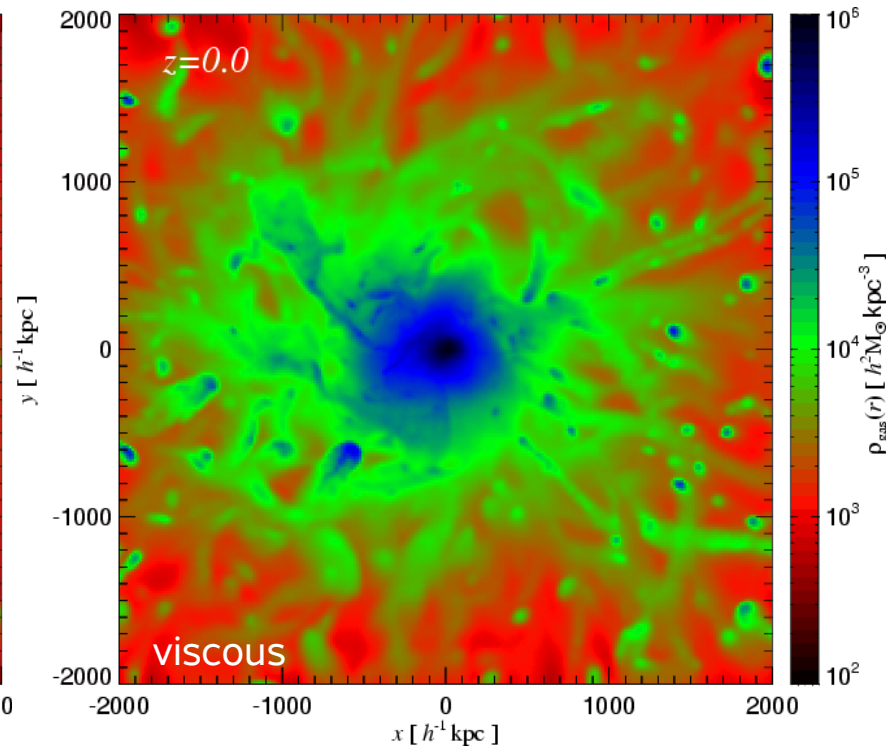
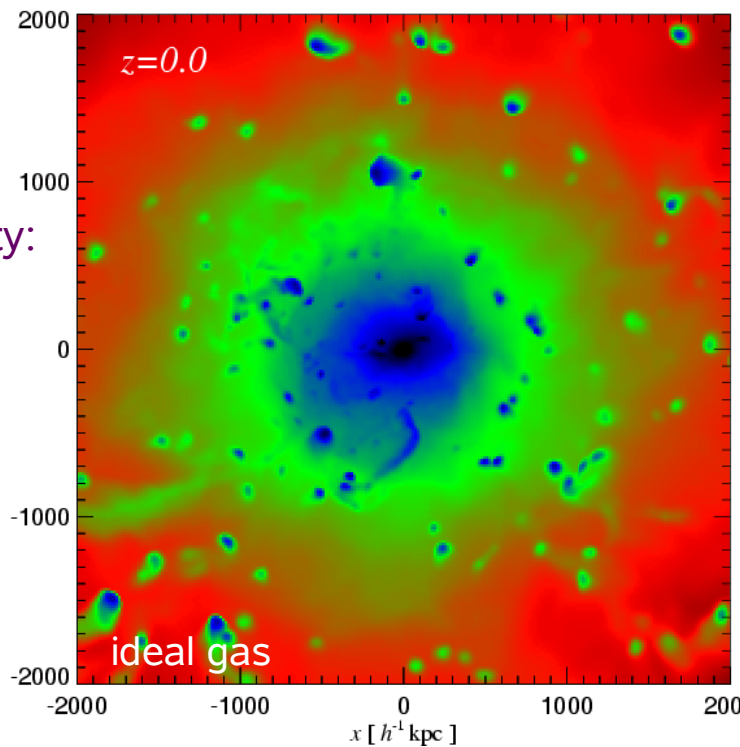
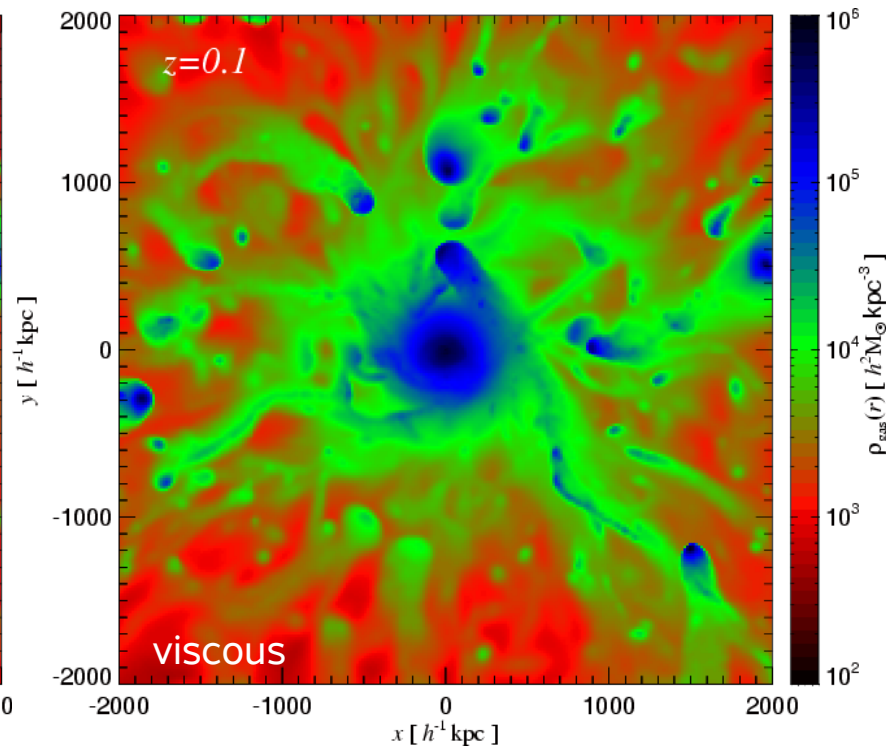
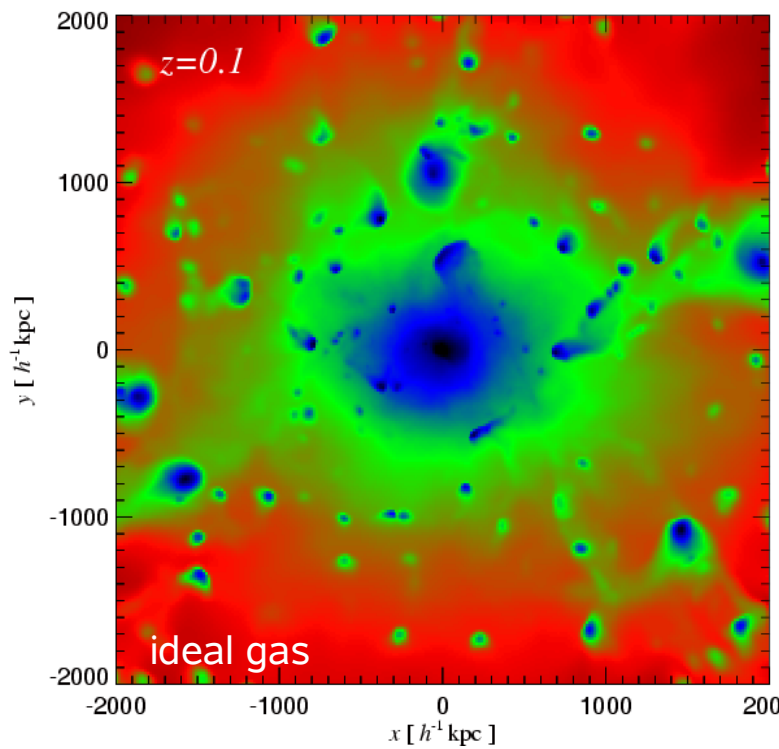
$$\left. \frac{dA_i}{dt} \right|_{\text{shear}} = \frac{1}{2} \frac{\gamma - 1}{\rho_i^{\gamma-1}} \frac{\eta_i}{\rho_i} \sigma_i^2$$

$$\left. \frac{dA_i}{dt} \right|_{\text{bulk}} = \frac{\gamma - 1}{\rho_i^{\gamma-1}} \frac{\zeta_i}{\rho_i} (\nabla \cdot \mathbf{v}_i)^2$$

# Viscous shear changes gas stripping during cluster assembly

## COMPARISON OF PROJECTED GAS DENSITY MAPS

Sijacki & Springel (2006)



Braginskii shear viscosity:

$$\eta = 0.406 \frac{m_i^{1/2} (k_B T_i)^{5/2}}{(Ze)^4 \ln \Lambda}$$



# Radiative transfer in SPH

# Different radiative transfer schemes have been proposed for SPH

## TRACING RAYS

Radiative transfer equation in comoving coordinates

$$\frac{1}{c} \frac{\partial I_\nu}{\partial t} + \frac{\hat{\mathbf{n}} \cdot \nabla I_\nu}{\bar{a}} - \frac{H}{c} \left( \nu \frac{\partial I_\nu}{\partial \nu} - 3I_\nu \right) = \epsilon_\nu - \kappa_\nu I_\nu$$

**Altay, Croft & Pelupessy (2008)**

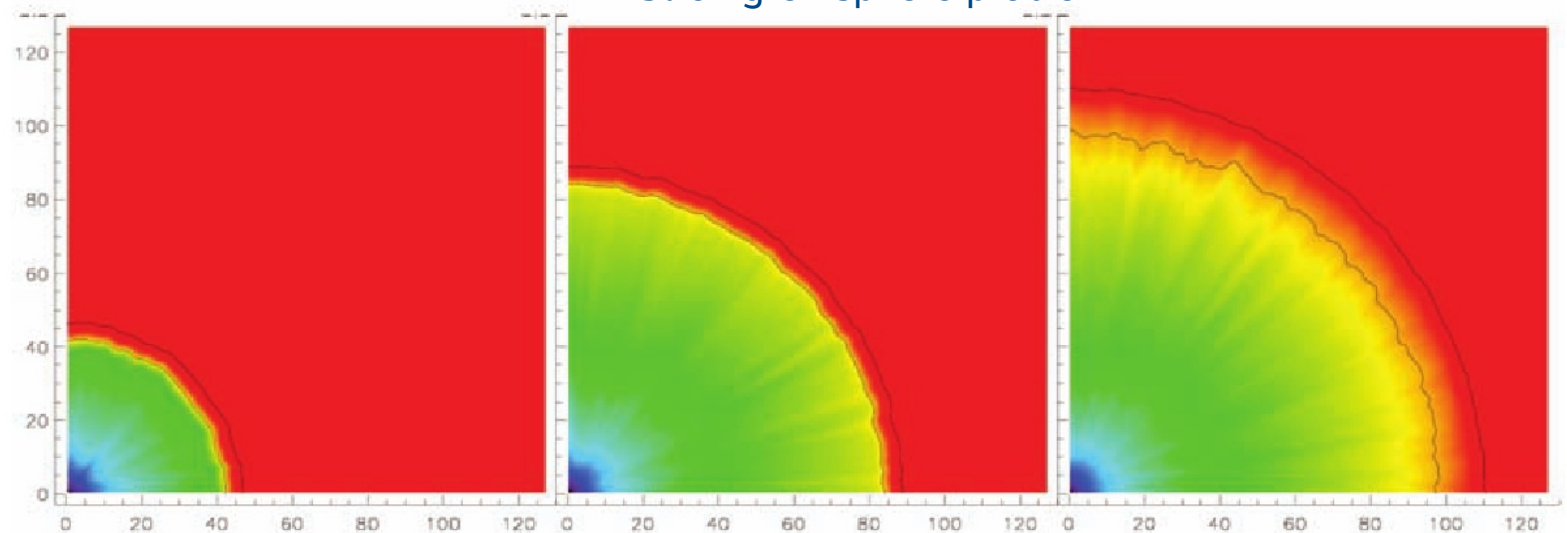
**SPHRAY** code (publicly available)

Individual rays are integrated in a Monte Carlo fashion through the SPH density field. The optical depth along a ray is calculated from the column density.

$$N_{\text{cd}} = \int_0^L \rho(\mathbf{r}) dl \approx \int_0^L \sum_{j=1}^N m_j W(r_{lj}, h_j) dl$$

Uses intersection tests motivated by computer graphics algorithms for efficiently evaluating SPH sum.

Strömgren sphere problem



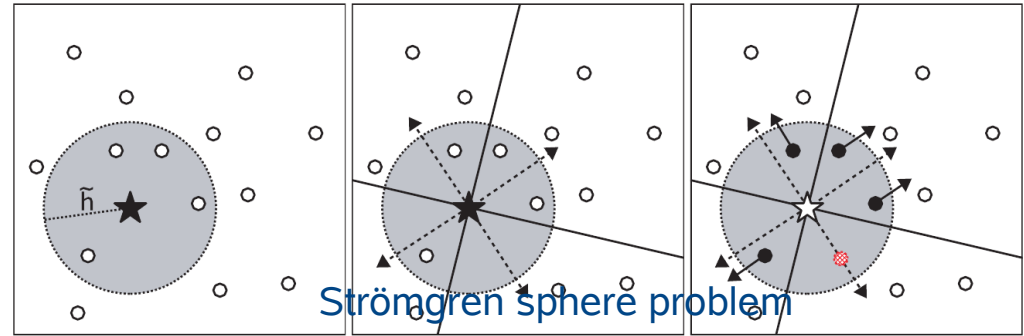
Different radiative transfer schemes have been proposed for SPH

**FOLLOWING THE RADIATION FIELD IN CONES**

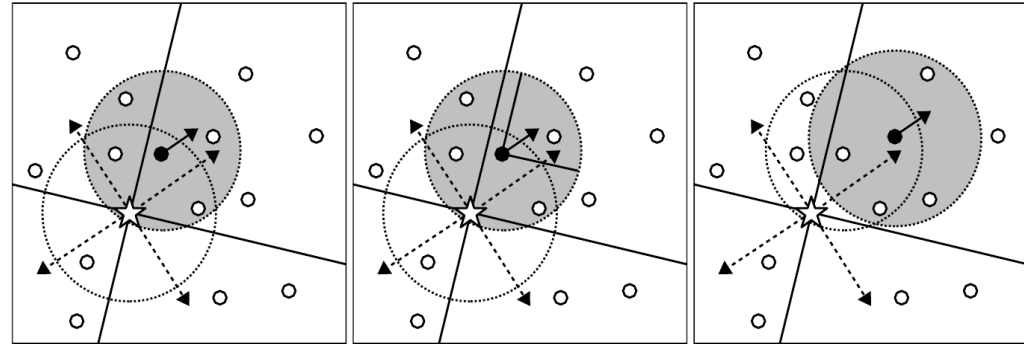
Pawlik & Schaye (2008)

TRAPHIC code

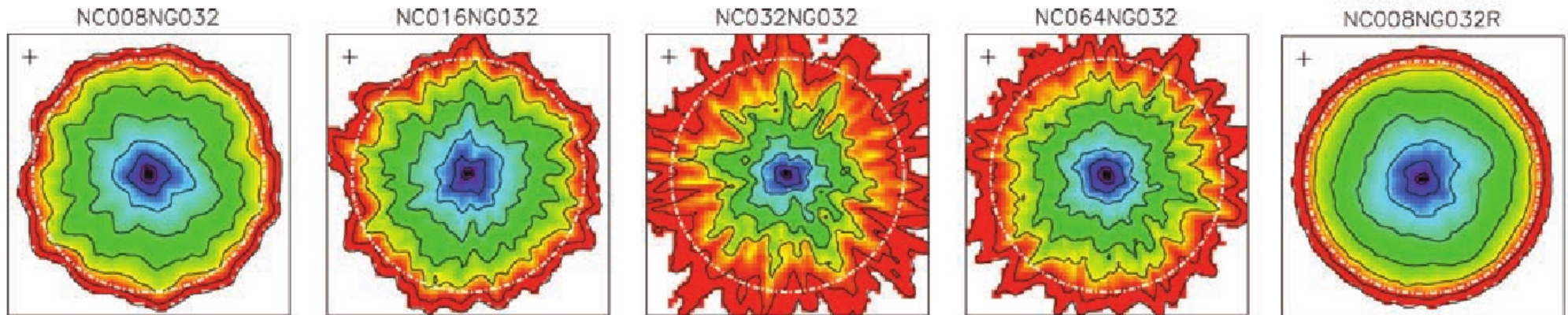
Source radiation is injected into emission cones



In transfer steps, radiation is received from cones and propagated into emission cones



Strömgren sphere problem



# Different radiative transfer schemes have been proposed for SPH

## MOMENT EQUATIONS

**Ansatz:** Take moments of the radiative transfer equation and achieve closure with an estimated Eddington tensor.

Mean intensity  $J_\nu = \frac{1}{4\pi} \int d\Omega I_\nu$

Radiation flux  $F_\nu^i = \frac{1}{4\pi} \int d\Omega n^i I_\nu$

Radiation pressure  $P_\nu^{ij} = \frac{1}{4\pi} \int d\Omega n^i n^j I_\nu$

$\frac{\partial J_\nu}{\partial t} = \frac{c}{a^2} \frac{\partial}{\partial x_j} \left( \frac{1}{\hat{k}_\nu} \frac{\partial J_\nu h^{ij}}{\partial x_i} \right) - c \hat{k}_\nu J_\nu + c j_\nu$

Eddington tensor  $h^{ij} = \frac{P^{ij}}{\text{Tr}(P)}$

Radiative transfer becomes an anisotropic diffusion problem.

Optically Thin Variable Eddington Tensor (OTVET) approximation (Gnedin & Abel 2001)

$$P^{ij} \propto \int d^3x' \rho_*(\mathbf{x}') \frac{(\mathbf{x} - \mathbf{x}')_i (\mathbf{x} - \mathbf{x}')_j}{(\mathbf{x} - \mathbf{x}')^4}$$

—▶ Can be calculated efficiently with a tree algorithm alongside gravitational force

Petkova & Springel (2009)

# Different radiative transfer schemes have been proposed for SPH

## OTVET SCHEME IN GADGET-3

Petkova & Springel (2009)

The anisotropic radiative diffusion problem can be discretized in SPH:

$$\frac{\partial N_i}{\partial t} = \sum_j w_{ij}(N_j - N_i) - c\hat{k}_i N_i$$

$$w_{ij} \equiv \frac{2cm_{ij}}{\kappa_{ij}\rho_{ij}} \frac{\mathbf{x}_{ij}^T \tilde{\mathbf{h}}_{ij} \nabla_i W_{ij}}{\mathbf{x}_{ij}^2}$$

photon number

Numerical stability requires an **implicit integration** (backwards Euler):

$$N_i^{n+1} = N_i^n + \Delta t \tilde{s}_i m_i + \sum_j \Delta t w_{ij}(N_j^{n+1} - N_i^{n+1}) - \Delta t c \sigma_0 n_{\text{HI}} N_i^{n+1}$$

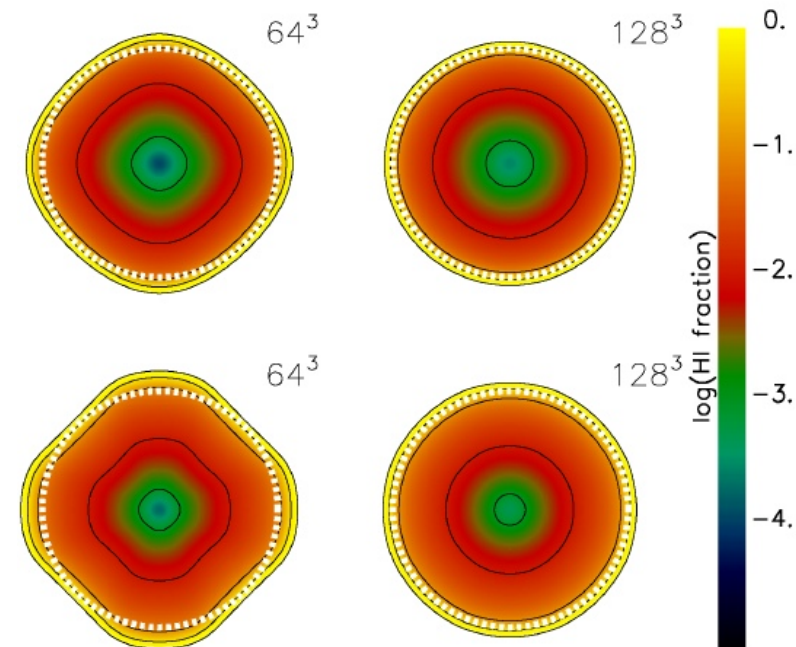
Finding the new radiation field is equivalent to solving a large linear system:

$$\mathbf{Ax} = \mathbf{b}$$

$$A_{ij} = \delta_{ij} \left( 1 + \sum_k \Delta t w_{ik} + \Delta t c \sigma_0 n_{\text{HI}} \right) - \Delta t w_{ij}$$

As the matrix is symmetric and positive definite, the system can be solved iteratively with the **conjugate gradient method**. Jacobi **preconditioning** can be used to speed up convergence.

Strömgren sphere problem



# Magnetic fields in SPH

It is possible to treat MHD in SPH, but  $\text{div}B$  errors remain problematic in the formulations proposed thus far

## SPH MHD FORMULATIONS

### (1) Direct discretization of the MHD equations in terms of $B$ Dolag et al. (1999)

Even when  $\text{div} B = 0$  initially, the errors usually blow up when the magnetic forces become comparable to thermal pressure forces.

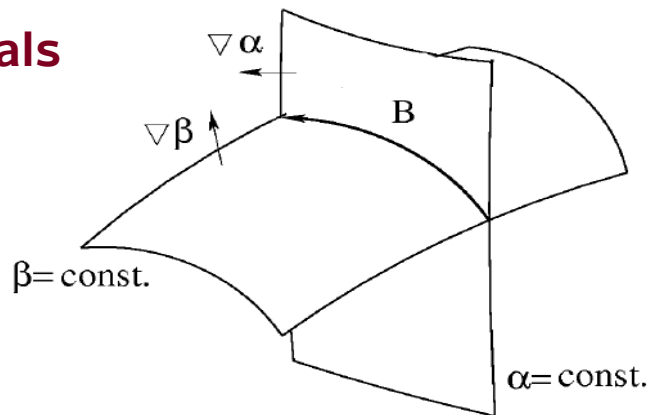
This needs to be controlled by field cleaning and/or smoothing methods, and a judicious choice of the SPH discretization.

### (2) Use of the Euler potentials

$$\mathbf{B} = \nabla\alpha \times \nabla\beta.$$

$\alpha$  and  $\beta$  effectively label field lines, and are simply advected with the flow in ideal MHD.

$$\frac{d\alpha_a}{dt} = 0 \quad \frac{d\beta_a}{dt} = 0$$



Rosswog & Price (2008)

- Euler potentials not unique for a given field, and not all fields can be represented
- Unclear how dissipation should be treated
- Higher-order derivatives give noisy magnetic forces
- Dynamo action and magnetohydrodynamic turbulence may be suppressed (Brandenburg 2009)

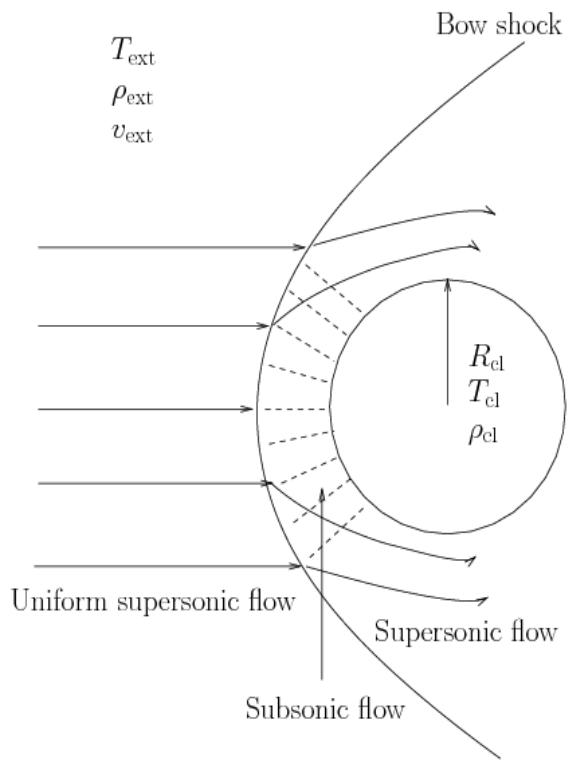
### (3) Use of the vector potential

# Fluid instabilities and mixing in SPH

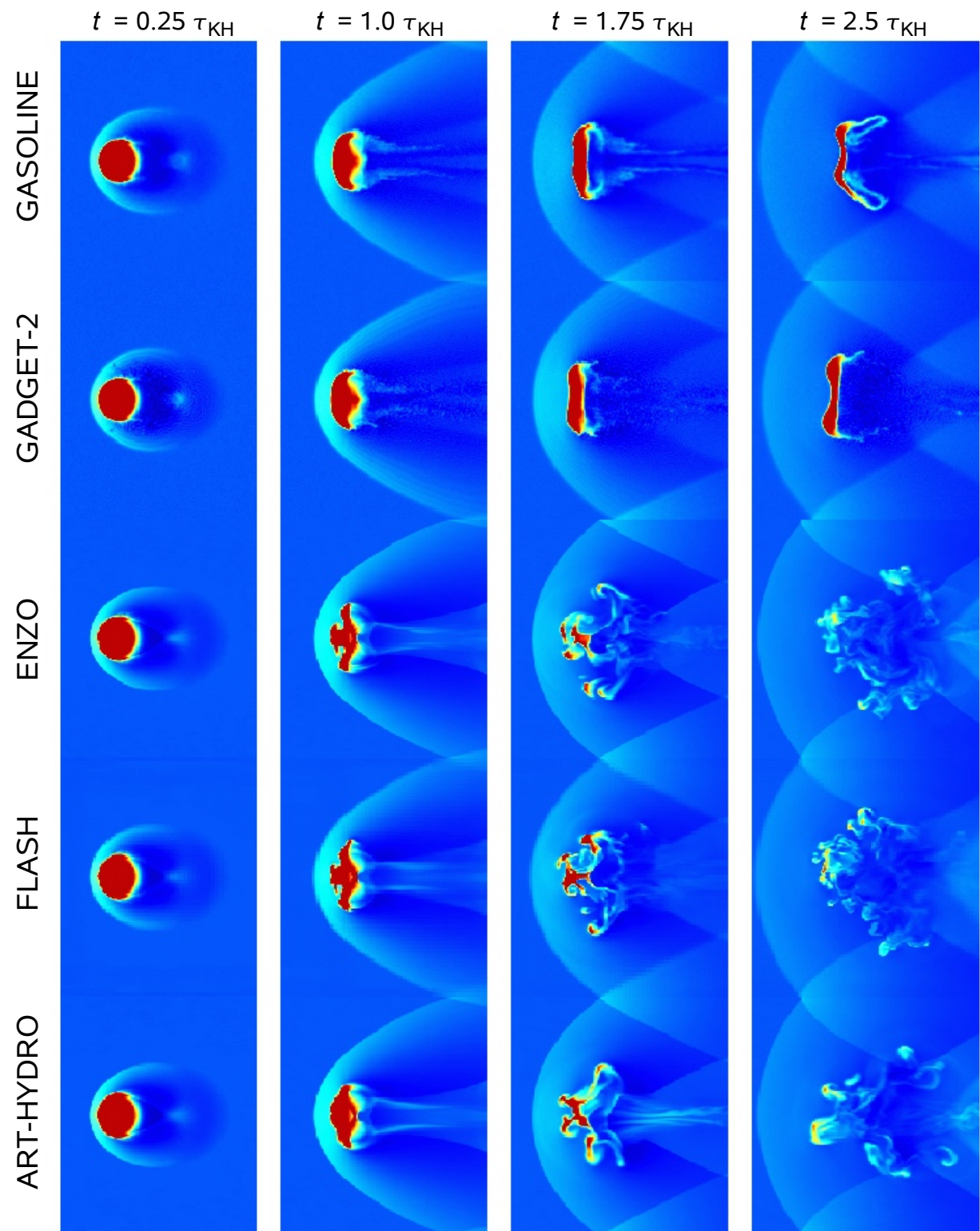


A cloud moving through ambient gas shows markedly different long-term behavior in SPH and Eulerian mesh codes

**DISRUPTION OF A CLOUD BY KELVIN-HELMHOLTZ INSTABILITIES**



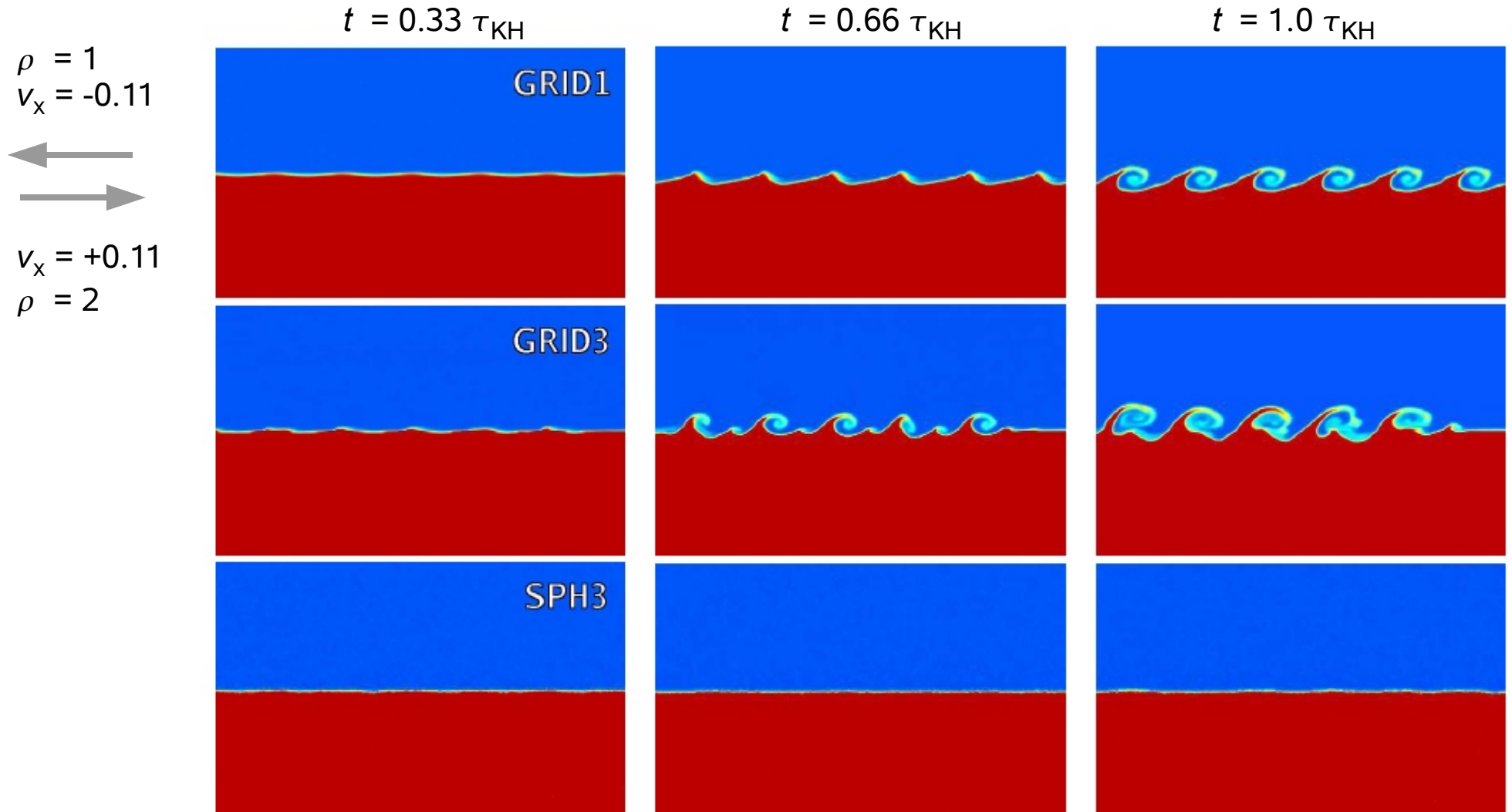
Agertz et al. (2007)



In SPH, fluid instabilities at contact discontinuities with large density jumps tend to be suppressed by a spurious numerical surface tension

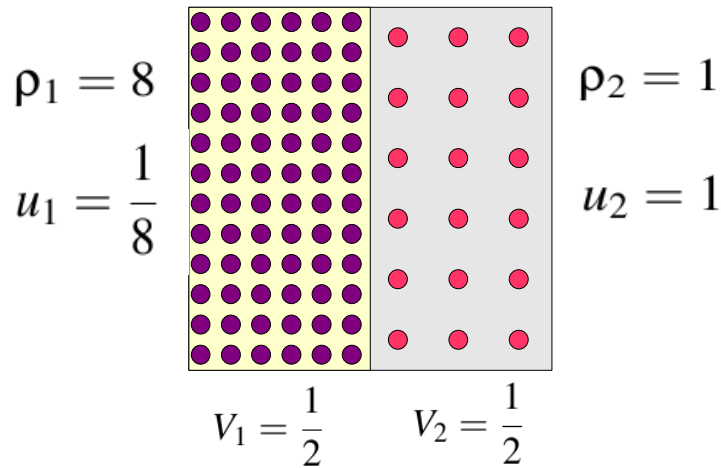
### KELVIN-HELMHOLTZ INSTABILITIES IN SPH

Agertz et al. (2007)



# Thought experiment on mixing

# A simple *Gedankenexperiment* about mixing in SPH



The pressure is constant:

$$P_1 = (\gamma - 1)\rho_1 u_1 = \frac{2}{3} \quad P_2 = P_1$$

The specific entropies are:

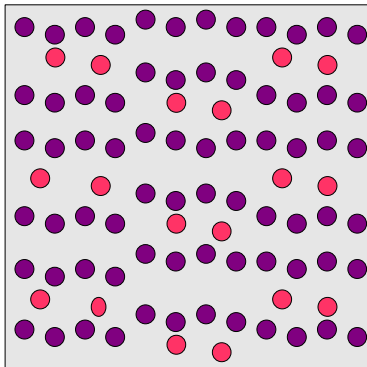
$$A_i = \frac{P_i}{\rho_i^\gamma} \quad A_1 = \frac{1}{48} \quad A_2 = \frac{2}{3}$$

Let's calculate the total thermal energy of the system:

$$E_{\text{therm}} = \int \frac{A\rho^{\gamma-1}}{\gamma-1} dm$$

$$E_{\text{therm}} = 1$$

We now mix the particles, keeping their specific entropies fixed:



All particles estimate the same mean density:

$$M_{\text{tot}} = \frac{9}{2} \quad \bar{\rho} = \frac{9}{2}$$

The thermal energy thus becomes:

$$E_{\text{therm}} = \frac{M_1 A_1 \bar{\rho}^{2/3}}{2/3} + \frac{M_2 A_2 \bar{\rho}^{2/3}}{2/3}$$

$$E_{\text{therm}} = \frac{5}{8} \left( \frac{9}{2} \right)^{2/3} \simeq 1.7$$

➡ This mixing process is energetically forbidden!

# What happened to the entropy in our *Gedankenexperiment* ?

In slowly mixing the two phases, we preserve the total thermal energy:

$$\text{Expect: } \quad \bar{u} = \frac{2}{9} \quad \bar{A} = \frac{2}{3} \frac{\bar{u}}{\bar{\rho}^{2/3}} \quad \bar{A} = \frac{2^{8/3}}{3^{13/3}} \simeq 0.054$$

The Sackur-Tetrode equation for the entropy of an ideal gas can be written as:

$$S = \frac{3}{2} \frac{k_B}{\mu} M \left[ \ln \left( \frac{P}{\rho^\gamma} \right) + \ln \left( \frac{2\pi\mu^{8/3}}{h^2} \right) + \frac{5}{3} \right]$$

If the mass in a system is conserved, it is sufficient to consider the simplified entropy:

$$\tilde{S} = M \ln A$$

When the system is mixed, the change of the entropy is:

$$\Delta\tilde{S} = M_{\text{tot}} \ln \bar{A} - (M_1 \ln A_1 + M_2 \ln A_2)$$

$$\Delta\tilde{S} \simeq 2.55 \geq 0$$

➡ Unless this entropy is generated somehow, SPH will have problems to mix different phases of a flow.

(Aside: Mesh codes can generate entropy outside of shocks – this allows them to treat mixing.)

New developments in SPH  
that try to address mixing

Artificial heat conduction at contact discontinuities has been proposed as a solution for the suppressed fluid instabilities

## ARTIFICIAL HEAT MIXING TERMS

Price (2008)

Wadsley, Veeravalli & Couchman (2008)

Price argues that in SPH every conservation law requires dissipative terms to capture discontinuities.

The normal artificial viscosity applies to the momentum equation, but discontinuities in the (thermal) energy equation should also be treated with a dissipative term.

**For every conserved quantity  $A$**

$$\sum_j m_j dA_j/dt = 0$$

**a dissipative term is postulated**

$$\left(\frac{dA_i}{dt}\right)_{\text{diss}} = \sum_j m_j \frac{\alpha_A v_{\text{sig}}}{\bar{\rho}_{ij}} (A_i - A_j) \hat{\mathbf{r}}_{ij} \cdot \nabla W_{ij}$$

**that is designed to capture discontinuities.**

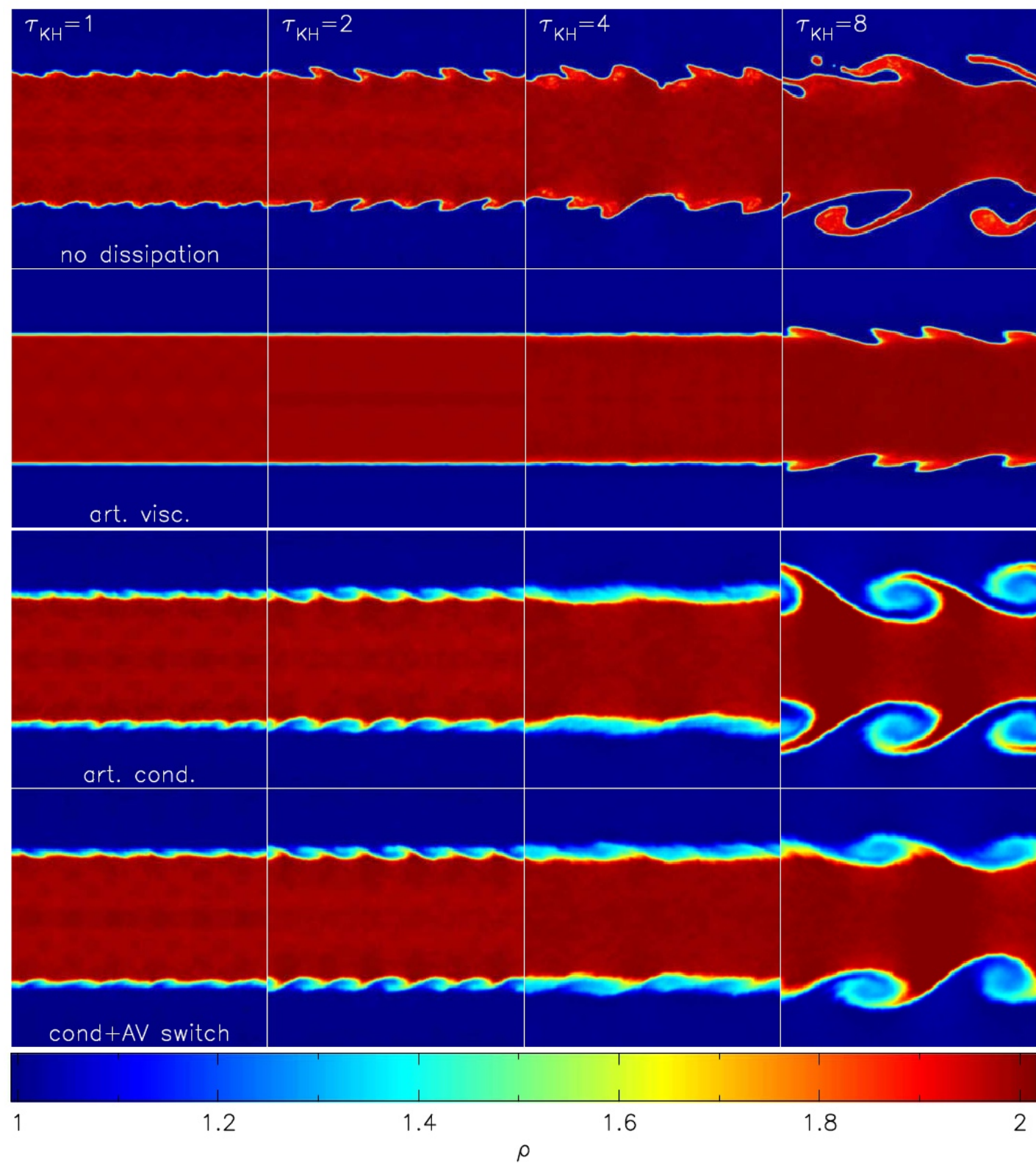
**This is the discretized form of a diffusion problem:**

$$\left(\frac{dA}{dt}\right)_{\text{diss}} \approx \eta \nabla^2 A$$

$$\eta \propto \alpha v_{\text{sig}} |r_{ij}|$$

Artificial heat conduction drastically improves SPH's ability to account for fluid instabilities and mixing

COMPARISON OF KH TESTS FOR DIFFERENT TREATMENTS OF THE DISSIPATIVE TERMS



Price (2008)



# Another route to better SPH may lie in different ways to estimate the density

## AN ALTERNATIVE SPH FORMULATION

“Optimized SPH” (OSPH) of [Read, Hayfield, Agertz \(2009\)](#)

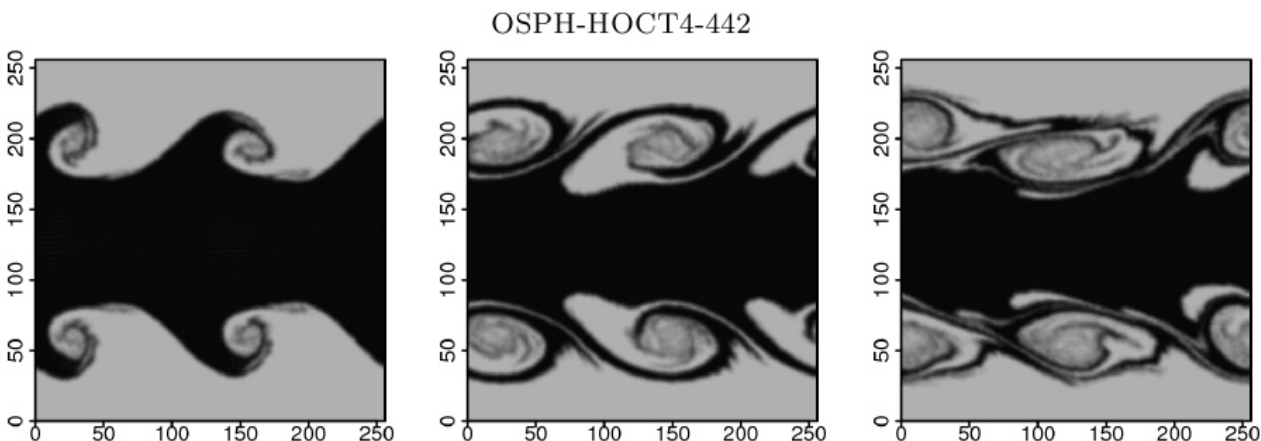
- Density estimate like Ritchie & Thomas (2001):

$$\rho_i = \sum_j^N \left( \frac{A_j}{A_i} \right)^{\frac{1}{\gamma}} m_j \bar{W}_{ij}$$

- Very large number of neighbors (442 !) to beat down noise

- Needs peaked kernel to suppress clumping instability

- This in turn reduces the order of the density estimate, so that a large number of neighbors is required.



RAMSES; 256 × 256 cells, no refinement, LLF Riemann solver

